

**MAKERERE**



**UNIVERSITY**

**COLLEGE OF ENGINEERING, DESIGN, ART  
& TECHNOLOGY**

**SCHOOL OF BUILT ENVIRONMENT**

**DEPARTMENT OF GEOMATICS & LAND  
MANAGEMENT**

**FINAL YEAR PROJECT REPORT**

**COMPARISON OF STANDARDIZED PRECIPITATION INDEX(SPI) AND  
VEGETATION HEALTH INDEX(VHI) IN DROUGHT MONITORING IN  
ISINGIRO DISTRICT**

**NAME: AINEMBABAZI SUZAN  
REGISTRATION NUMBER: 18/U/22939/PS  
SUPERVISED BY: DR. BRIAN MAKABAYI**

**Submitted in partial Fulfilment of the Requirements of the Award of a Bachelor's degree in  
Geomatics and Land Management.**

**SEPTEMBER 2022**

**DECLARATION**

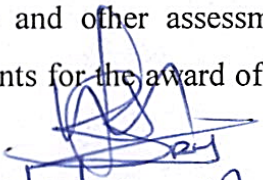
I AINEMBABAZI SUZAN declare that this Research dissertation is my work and I have correctly acknowledged the work of others. I, therefore, deny any plagiarism and other assessment irregularities as I submit this report in partial fulfilment of the requirements for the award of the Degree in Bachelor of Science in Land Surveying and Geomatics.

Signature:  .....

Date..... 14/11/2022 .....

AINEMBABAZI SUZAN

18/U/22939/PS

  
Signature: 11/11/2022 .....

Date.....

DR. BRIAN MAKABAYI

Department Supervisor

### **ACKNOWLEDGEMENT**

I believe no amount of human effort can achieve any success by itself. It is only logical to admit that all success no matter the size, is attributed to Our Father who art in Heaven. To You God, receive my thanks for providence in all its forms, notwithstanding the good health, that together enabled me to develop this idea. I would like to extend my sincere thanks to my supervisor Dr. Brian Makabayi for the constant guidance as I made this research. I am delighted and truly grateful for the support. May God bless you.

## ABSTRACT

Drought is a recurring and most complex weather-related natural phenomenon, affecting vast areas and communities around the world every year due to its slow onset and cascading effects. Droughts are common in Uganda's cattle corridor, but there is limited information on their occurrence and severity. The magnitude and pattern of drought can be measured with various drought indices using remote sensing and meteorological data. Many indices are used to monitor drought events. However, different indices have different data requirements and applications. Hence, evaluating their applicability will help to characterize drought events and refine the development of effective drought indices. The characteristics of drought events from 2000 to 2020 were compared using Standardized Precipitation Index and Vegetation Health Index at a five-year interval.

Drought was assessed using Landsat 8 OLI and 7 ETM temporal images based on Vegetation Health Index for the years; 2000, 2005, 2010, 2015 and 2020. In addition, SPI was utilized together with DrinC software and meteorological (monthly precipitation) data from the Uganda National Meteorological Authority to compute, determine and graphically illustrate trend in drought severity from 1990 to 2020 at various time scales (3,6 and 12 month).

Vegetation Health Index and Standardized Precipitation Index were used to identify the temporal and spatial drought patterns as derived from the study of a 20-year time period. The analysis revealed that 2000 and 2015 were the driest years. Using SPI, the southeastern and northwestern parts of the Isingiro district are the areas that are susceptible to drought and while using VHI, it was the northwestern, southwestern and southwestern parts of Isingiro are the areas that are susceptible to drought. SPI works well when there is an even distribution of weather stations in the area.

SPI-3 and VHI-2010 had the lowest correlation of 0.105 at the 3-month time scale and the highest correlation was in 2000(0.541) and 2015(0.659). VHI showed more areas affected by drought compared to SPI. The comparative analysis of the two indices indicated that VHI and SPI are highly correlated in the years 2000 and 2015. Drought analysis based on these indices showed that for drought assessment VHI can be used to depict drought condition of the study area more realistically. The results of this comparison show that 12-month scale of SPI and VHI have a higher correlation.

# Table of Contents

<b>DECLARATION</b> .....	2
ACKNOWLEDGEMENT.....	3
LIST OF ABBREVIATIONS .....	9
CHAPTER ONE: INTRODUCTION.....	10
1.1 Background .....	10
1.2 Problem Statement.....	11
1.3 Objective .....	12
1.3.1 Main objective .....	12
1.3.2 Specific objectives.....	12
1.4 Justification .....	12
1.5 Study Area.....	13
CHAPTER TWO: LITERATURE REVIEW .....	14
2.1 Introduction .....	14
2.2 Definition of drought .....	14
2.3 The different types of drought.....	15
2.3.1 Meteorological drought .....	16
2.3.2 Agricultural drought.....	16
2.3.3 Hydrological drought .....	16
2.3.4 Socio-economic drought.....	17
2.4 Remote Sensing and Geographical Information System (GIS).....	17
2.5 The different drought indices used in drought risk assessment.....	19
2.5.1 Meteorological drought indices.....	19
2.5.2 Palmer Drought Severity Index (PDSI) .....	19
2.5.3 Standardized Water Supply Index (SWSI) .....	20
2.5.4 Crop Moisture Index .....	20
2.5.5 Standardized Precipitation Index.....	21
2.6 Satellite based drought indices for Agricultural drought characterization .....	22
2.6.1 Vegetation Condition Index (VCI).....	22
2.6.2 Temperature Condition Index (TCI) .....	23
2.6.3 Normalized Difference Vegetation Index (NDVI) .....	24
2.6.4 Vegetation Health Index .....	26

2.7 Land Surface Temperature (LST).....	27
2.7 LST estimation.....	27
2.7.1 The Qin et al.'s mono-window algorithm .....	27
2.7.2 Single channel algorithm.....	28
2.7.3 Radiative transfer equation .....	28
2.8 The methods used in previous studies .....	29
2.9 Digital image processing .....	32
2.9.1 Image pre-processing.....	32
2.9.2 Radiometric and Geometric correction .....	32
CHAPTER THREE: METHODOLOGY.....	34
3.1 Data collection .....	35
3.2 Data processing.....	35
3.2.1 Image pre-processing.....	35
3.2.2 Clipping and masking to study area .....	36
3.3 Computation of Normalized Difference Vegetation Index (NDVI) .....	36
3.4 Computation of Vegetation Condition Index (VCI) .....	36
3.5 Computation of Land Surface Temperature .....	36
3.6 Computation of Temperature Condition Index (TCI).....	37
3.7 Computation of Vegetation Health Index.....	37
3.8 Computation of Standardized Precipitation Index (SPI) .....	37
3.9 Generation of maps from SPI and VHI data .....	39
CHAPTER FOUR: RESULTS AND DISCUSSIONS.....	40
4.1 Introduction .....	40
4.2 Results and Discussion .....	40
4.2.1 Drought Severity and frequency.....	40
4.2.2 Standardized Precipitation Index (SPI) drought maps .....	43
4.2.3 Vegetation Health Index (VHI) drought maps.....	46
4.2.4 Analysis of the relationship between SPI and VHI .....	50
CHAPTER FIVE: CONCLUSION AND RECOMMENDATION .....	51
5.1 Introduction .....	51
5.2 Conclusion.....	51
5.3 Recommendations .....	51
REFERENCES.....	52

## List of Figures

Figure 1: Study Area.....	13
Figure 2: Shows the methodology flow chart .....	34
Figure 3: Interface of DrinC software.....	39
Figure 4:SPI results at 3-month time scale .....	40
Figure 5:SPI results at 6-month time scale .....	41
Figure 6: SPI results at 12-month time scale .....	42
Figure 7: SPI maps of Isingiro district for the years 2000 and 2005 .....	43
Figure 8: SPI maps of Isingiro district for the years 2010,2015 and 2020 .....	44
Figure 9: VHI maps of Isingiro district for the years 2000 and 2005 .....	46
Figure 10: VHI maps of Isingiro district for the years 2010, 2015 and 2020 .....	47
Figure 11: Statistics from change detection for SPI.....	49
Figure 12: Statistics from change detection for VHI .....	49

## **List of tables**

Table 1:Category of SPI based on range values (source:(Chopra, 2006) .....	22
Table 2: Category of VHI based on range values (source: (Kogan, 2002)).....	27
Table 3: Area and Percentage area of drought for the years 2000, 2005, 2010, 2015 and 2020 for SPI....	48
Table 4: Area and Percentage area of drought for the years 2000, 2005, 2010, 2015 and 2020 for VHI...	48
Table 5: Correlation coefficients between VHI and SPI.....	50



## LIST OF ABBREVIATIONS

CMI	Crop Moisture Index
GIS	Geographical Information System
LULC	Land Use and Land Cover
NDVI	Normalized Difference Vegetation Index
PDSI	Palmer Drought Severity Index
RS	Remote Sensing
SPI	Standardized Precipitation Index
SWSI	Standardized Water Supply Index
TCI	Temperature Condition Index
USGS	United States Geological Survey
VCI	Vegetation Condition Index
TCI	Temperature Condition Index
VHI	Vegetation Health Index
IDW	Inverse Distance Weighting
Drinc	Drought Index Calculator

## CHAPTER ONE: INTRODUCTION

### 1.1 Background

Droughts occur naturally but climate change has generally accelerated the hydrological processes to make them set in quicker and become more intense with many consequences (Karnieli et al., 2010). Anthropogenic activities are causing current climate change and variability, which are increasing greenhouse gas concentrations in the atmosphere at an alarming rate, resulting in severe temperatures, droughts and flooding. Although drought is a natural occurrence, human activities such as deforestation, overgrazing, and inefficient farming methods, among others, can exacerbate its effects by reducing water retention of soil (ECA, 2007). As a result, these are causing an increasing occurrence of flooding and drought which are challenges for Africa due to a lack of financial, technical, and institutional capacity to deal with the consequences (Gemedo & Sima, 2015). Water availability, accessibility and demand in Africa may be further strained as a result of the change. Due to many negative impacts associated with Global climate change, there is an increased focus on the occurrence of and preparation for climate-related extremes and catastrophes (Christenson et al., 2014).

Drought has become a prime worldwide concern owing to its severe effect on agricultural productivity both animal and crop husbandry and indirect effect on employment (Dutta, et al., 2015). Prolonged multiyear drought has caused significant damages both in the natural environment as well as in the development of the human society. The annual estimate for the cost of drought in the United States ranges from 6 to 8 billion dollars (Schubert, et al., 2007). In China, the amount of loss caused by drought ranks the first in the list of all natural hazards (Song, et al., 2003). Drought is arguably the biggest threat resulting from climate change with its impacts being global (Pearce, 2015). According to the World Bank report of 2016, Uganda's population being predominantly rural is limited in its ability to handle production shocks (Maher, 2017). Drought continues to be a big setback in agricultural activities especially if not well prepared for (Akwango, et al., 2017).

Unlike sudden disasters, drought-related disasters develop gradually over time lasting for many years and having devastating effect on life and livelihoods (Prasanna, 2018; Mills et al., 2016). In severe circumstances it results to inadequate water for plants, animals, and humans. Drought can lead to food insecurity, starvation, malnutrition, diseases, and population displacement (Muller, 2014). According to history, about 20% of the earth's geographical surface has ever suffered

drought at any given moment. Drought-stricken areas have expanded from 1% to 3% of the planet's surface in the last decade, and the situation is set to worsen. Particularly in Africa where agriculture is mostly rain fed especially in the East African economies, droughts have persistently led to widespread crop failure, food shortages, economic and even humanitarian crises (Nimusiima et al. 2018). Kenya's, Uganda's, and Tanzania's gross domestic product (GDP) are accounted for by the agricultural sector in proportions of 51%, 42% and 25% respectively. With this and the tendency of an increasing frequency and intensity of these events, damage to the agricultural sector leaves the region exposed to the risk of famine (Mwangi et al., 2014; Adede et al., 2015).

In Uganda, recent severe droughts registered have had negative impacts on the water sector, agriculture and all sectors of the economy (Uganda National Climate Change Policy, 2015; MAAIF & MWE, 2017). The Ugandan government on the other hand has taken a range of steps to resolve the impact of emergencies and disasters on the population, including national disaster preparedness and management strategy and the Sustainable Development Goals. Uganda has recently created a risk and threat atlas to aid in disaster identification and mitigation (United Nations Development Programme, 2021).

Despite public awareness of the problem, there is still a scarcity of information on drought, particularly on its prevalence and severity (Mulinde et al., 2016). Droughts are common in the cattle corridor region, according to (Makuma-Massa et al., 2012) who forecasts an increase in frequency and severity. As a result, several mitigation measures have been implemented to mitigate the effects. But these have not been efficient at addressing the information gap of the drought severity and its associated impacts. A lot of research has been conducted to monitor drought using several drought indices that use remote sensing data. This research therefore seeks to assess the performance of using Standardized Precipitation Index(SPI) and the Vegetation Health Index (VHI) for monitoring drought in Isingiro district so as to have an alternative index to monitor drought.

## **1.2 Problem Statement**

Drought is a complex phenomenon and it is still a problem for many countries. Many indices are used to monitor drought events. However, different indices have different data requirements and applications. Hence, evaluating their applicability will help to characterize drought events and refine the development of effective drought indices. Isingiro district is mainly affected by

agricultural drought and SPI is the most widely used and recognized index by World Meteorological Organization for monitoring agricultural drought. Most studies have monitored agricultural drought using SPI that is calculated based on precipitation observations from stations that are unevenly distributed. The existing meteorological dataset has a series of gaps and cannot be filled and used for drought assessment (Mfitumukiza et al., 2017). The gaps are attributed to vandalism and subsequent system breakdowns. SPI needs continuous and long term precipitation data to give more representative results of the drought in the area. Meteorological data in Uganda is commercial and expensive. Therefore, there is need to use an index that employs other parameters whose data is easy to acquire, cheap and give reliable results as would be provided by SPI and can be relied on to monitor agricultural drought in Isingiro district to aid in the development of better and informed management plans in assessing drought and its consequences. This research seeks to compare the results of VHI and SPI so as to establish the applicability of VHI in agricultural drought assessment.

### **1.3 Objective**

#### **1.3.1 Main objective**

To assess the performance of SPI and VHI in drought monitoring in Isingiro district.

#### **1.3.2 Specific objectives**

- To determine spatial temporal variation of drought from 2000-2020
- To determine the relationship between SPI and VHI

### **1.4 Justification**

Apart from loss to agriculture, droughts have major negative effects, including land degradation, loss of life, and livestock. These challenges can increase drastically when drought is not properly managed. Information about drought occurrence and severity can help the government and authorities mitigate drought-related impacts. Since droughts have been a recurring feature of the Isingiro climate, the district needs drought analysis information. The present study seeks to provide information on drought severity in Isingiro district to the locals, policy makers and government authorities to cope with its disastrous effects can formulate thereby informed management plans.

## 1.5 Study Area

Isingiro District is a District in South Western Uganda boarded by Kiruhura District to the north, Rakai District to the east, the Republican of Tanzania to the south, Ntungamo District to the west, and Mbarara District to the northwest. Isingiro the chief town of the District is located approximately 35 kilometers by road, southeast of the city of Mbarara, the main metropolitan area in Ankole sub-region. Isingiro District has 21 Sub-counties and 9 Town Councils, 131 parishes and 899 Villages by July 2020. It lies between the altitude of 1200m – 1810m above sea level. Areas west of the District around Nyakitunda, Nyamuyaja, Kabingo and Kabuyanda hills have the highest altitudes up to 1810m towards Mbarara and Ntungamo District boarder. The low altitudes are along areas east of the District around Endiizi, Rushasha sub counties bordering with Rakai District and the lowest being at the main L. Nkivale water body in Rugaga Sub-County. Its Land area is approximately 3010 sq. Km and it is at 1800 meters above sea level.

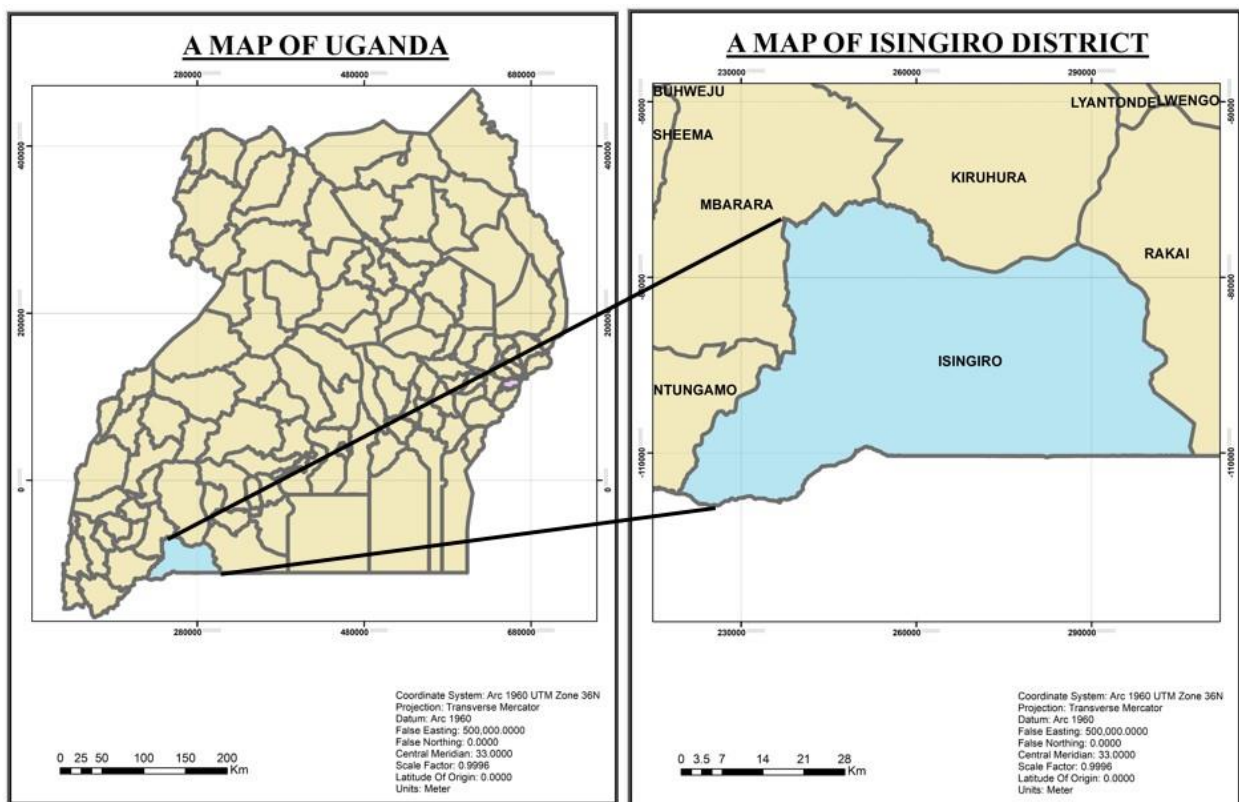


Figure 1: Study Area

## CHAPTER TWO: LITERATURE REVIEW

### 2.1 Introduction

The literature review will examine the different areas of drought assessment research that are relevant to this study's goals. It includes data gathered from textbooks, journals, reports, and Internet, among other places. This chapter will try to harmonize the work of various scholars from various parts of the world in relation to Isingiro district in Uganda, where drought is a concern.

### 2.2 Definition of drought

Many people believe that drought is the most complicated but least known of all-natural hazards, affecting more people than any other threat. It is distinct from other natural disasters such as hurricanes, tropical cyclones, and earthquakes, which occur over finite time periods and cause visible damage as it often builds up slowly over a long period of time and can last for years after the event has ended, leading to the term "creeping phenomenon" (Wilhite, 2021). The phenomenon is difficult to research due to its slow onset and inability to discern when it began and when it ended (Abuzar *et al.*, 2017). Drought does not have a generally accepted description, owing to the fact that it must be described in terms of the characteristics of each climatic regime (Van Loon, 2015). Below are some of the descriptions of drought as obtained from different drought research;

A drought is an extended period of months or years when a region notes a deficiency in its water supply, whether surface or underground water especially due to existence of a precipitation level that is below average (Achite *et al.*, 2022)

Bayissa *et al.* (2018) define drought as "an abnormally dry condition that persists for a long period of time". However, drought happens with different frequency in practically every part of the globe, in all sorts of economic systems, and in both developed and developing countries, therefore the methodologies used to characterize it must take into account geographical and ideological distinctions. As a result, in areas where precipitation is seasonal and lengthy intervals without rain are common, such a definition is unrealistic.

Drought can also broadly be defined as a long-term average condition of the balance between precipitation and evapotranspiration in a particular area, which also depends on the timely onset of monsoon as well as its potency (Wilhite *et al.*, 1987).

Drought refers to a deficiency of precipitation over an extended period, resulting in a water shortage that causes extensive damage to crops, living as well as non-living things (Bera *et al.*, 2018). This embodies the impact aspect though realistically; definitions of drought must comprise both region and application of specific aspects.

Drought refers to lack of rainfall as great as so long continued to affect injuriously the plant and animal life of a place and to deplete water supplies both for domestic purposes and the operation of power plants especially in those regions where rainfall is normally sufficient for such purposes (Dracup, et al., 1980).

The UNDP (2008) define drought as “the naturally occurring phenomenon that exists when precipitation has been significantly below normal recorded levels, causing serious hydrological imbalances that adversely affect land resource production systems”. However, Drought should not be viewed as merely a physical or natural phenomenon. Rather, drought is the result of an interplay between a natural event and the demand placed on water supply by human-use systems (Wilhite et al, 2000) that is to say, in reality, drought has both a natural and social component.

All the above definitions have one thing in common “water deficit over an extended period of time”. (Wilhite et al, 1987) concluded that definitions of drought should reflect a regional bias since the water supply is largely a function of the climatic regime. Therefore, drought refers to a deficiency of water over an extended period of time with high impacts on the environment and agriculture in a given region. This study will adopt this definition.

Drought is usually caused by increasing temperatures and altered precipitation patterns. Drought leads to a decrease in rainfall and soil moisture which eventually affects agricultural production (Sruthi and Aslam, 2015). Drought monitoring and assessment can be done more accurately with the help of geospatial techniques like remote sensing (Sruthi and Aslam, 2015).

### **2.3 The different types of drought**

Droughts are grouped into four main types and are defined according to disciplinary perspectives (Heim, 2002). Meteorological drought, hydrological drought, socio-economic drought, and agricultural drought are discussed in detail below;

### **2.3.1 Meteorological drought**

Meteorological drought is usually defined by a precipitation deficiency threshold over a predetermined period of time (Sciences, 2012). Since the atmospheric conditions that result in a lack of precipitation are climate regime dependent, meteorological drought concepts are considered area-specific (Wilhite, 2021). The standard precipitation index (SPI), standard precipitation evapotranspiration index (SPEI), percentage of normal rainfall, and Palmer Drought Severity Index are some of the indices and methodologies used to describe meteorological drought. The SPI is currently the most used index worldwide to measure meteorological droughts and there on for this research.

### **2.3.2 Agricultural drought**

Agricultural drought is measured in terms of deficiency in soil moisture, rainfall, ground water and reduction in crop yield (Abuzar *et al.*, 2017). Drought in agriculture refers to an imbalance in the water content of the soil during the growing season which is affected by other factors such as crop water requirements, water-holding capacity and evaporation rate is largely dependent on rainfall amount and distribution. Since soil moisture supplies are often quickly depleted, agriculture is typically the first economic sector to be affected by drought particularly if the time of moisture shortage is associated with high temperatures and windy conditions (Wilhite, 2021). The Soil Moisture Percentile (SMP), Normalized Difference Vegetation Index (NDVI), Crop Moisture Index (CMI), Temperature Condition Index (TCI), Vegetation Condition Index (VCI), Vegetation Health Index (VHI), Normalized Soil Moisture (NSM), and Standardized Soil Moisture Index (SSI) are some of the most commonly used agricultural drought indicators. Agricultural drought usually precedes meteorological drought (Hao *et al.*, 2018)

### **2.3.3 Hydrological drought**

Hydrological drought refers to a duration of insufficient surface and subsurface water supplies for existing water uses of a given water resources management system. For hydrologic drought analysis, streamflow data has been commonly used. Geology is one of the key factors affecting hydrology, according to regression studies linking droughts in stream flow to catchment properties (Belal *et al.*, 2014). It also happens when there is a significant shortfall in surface runoff below normal conditions or when groundwater sources are depleted. As a result of the drought, the availability of water for irrigation, hydroelectric power generation, and other household and



industrial uses is reduced (Sciences, 2012). This could last for a long time after a meteorological drought has passed.

#### **2.3.4 Socio-economic drought**

Socio-economic drought is the final phase of drought that occurs when the demand for an economic good exceeds supply as a result of a weather-related shortfall in water supply (Belal *et al.*, 2014). It represents the impact of drought on human activities, including both indirect and direct impacts. This relates to a meteorological anomaly or extreme event of intensity and duration outside the normal range of events taken into account by enterprises and public regulatory bodies in economics (Sciences, 2012).

#### **2.4 Remote Sensing and Geographical Information System (GIS)**

Drought forecasting plays an important role in the planning and management of water resource systems (Karthika, et al., 2017). The identification of drought extent at administrative levels is an important program to evaluate the probability of drought occurrence and its severity especially to increase food security (Sruthi and Aslam, 2015). Early indication of possible drought can help to set out drought mitigation strategies and measures in advance (Karthika, et al., 2017). Impacts due to drought can be mitigated, if they are detected in advance through measures and monitoring.

Modern technologies such as Remote Sensing and Geographic Information Systems (GIS) have proved to be useful in studies relating to environmental resources most especially drought risk assessment. Drought can be monitored effectively over large areas using remote sensing technology (Sruthi and Aslam, 2015).

Remote sensing, according to the United States Geological Survey (USGS) is the method of detecting and tracking an area's physical characteristics by measuring its reflected and emitted radiation from a distance. Sensors with several spectral bands are placed on planes or satellites. A satellite orbits the Earth and explores the entire surface in a few days, returning to the same location at regular intervals to replicate the survey. The spectral bands used by these sensors span the visible to microwave spectrum (Jeyaseelan, no date).

Geographic Information System (GIS) is a computer-based method for mapping and evaluating objects that exist and events that occur on Earth, according to the Environmental Systems Research

Institute (ESRI). It entails capturing, storing, verifying, and displaying data about locations on the Earth's surface

The detection, monitoring and mitigation of the disaster and its effects requires relevant information regarding the disaster in real time and continuous data generation. Since disasters that cause huge social and economic disruptions normally affect large areas and are linked to global change, it is not possible to effectively collect continuous data on them using conventional methods. Remote sensing tools offer excellent possibilities of collecting this data. (Chopra, 2006). This allows continuous information to be obtained and distributed over wide areas using sensors that operate in several spectral bands and are installed on aircraft or satellites (Jeyaseelan, no date; Belal *et al.*, 2014).

Remote sensing and GIS plays an important role in detecting, assessing and managing droughts as they offer up to date data on spatial and temporal scales that can help alleviate the effects of drought (Abuzar *et al.*, 2019). Geographical Information Systems help to process Remote Sensing observations from satellites in a spatial format of maps and provide the spatial visualization of information of natural resources thus enabling easy identification, monitoring and assessment of droughts (Jeyaseelan, no date).

Remote sensing also serves as a great communication tool, allowing for coverage of inaccessible areas. As a result, remote sensing techniques are being used to monitor disasters at key stages such as before, during, and after the case. Most importantly this technology is being used to gather baseline data against which future changes can be compared as seen in this study.

Geographical Information System enables a meteorological station to connect to it and keep receiving meteorological information directly entered into GIS, and then these data managed and analyzed uniformly by the system database (Belal *et al.*, 2014).

Drought risk assessment has been significantly improved by advances in the fields of GIS and remote sensing (RS) over the last four decades. Because much of the data needed for drought risk assessment has a spatial dimension and changes over time, the use of GIS and RS is important (Belal *et al.*, 2014).

## **2.5 The different drought indices used in drought risk assessment**

### **2.5.1 Meteorological drought indices**

Many drought indices have been established and used by meteorologists and climatologists over the years to detect the potential for drought occurrence and severity around the world (Mlenga, Jordaan and Mandebvu, 2019). There are many indicators that calculate how much precipitation has deviated from historically defined averages over a given period of time. Palmer Drought Severity Index (PDSI), Crop Moisture Index (CMI), Standardized Precipitation Index (SPI), and Surface Water Supply Index are some of the most commonly used drought indices for Meteorological drought monitoring, forecasting, and water resource management (Himanshu, Singh and Kharola, 2015).

### **2.5.2 Palmer Drought Severity Index (PDSI)**

Palmer (1965) created the PDSI with the aim of measuring the accumulated departure in surface water balance or moisture supply so that comparisons using the index could be made between locations and between months. This has also been widely used to investigate variations in aridity in present and past climates. The index is a meteorological drought index that responds to weather conditions that are unusually dry or wet (Agwata, 2014). The PDSI is measured using weather data such as precipitation and temperature, as well as the soil's local Available Water Content (AWC). All of the basic elements of the water balance equation, including evapotranspiration, soil 12 recharge, runoff, and moisture loss from the surface layer, may be calculated using the inputs. Human influence on the water balance, such as irrigation, are not taken into account (Agwata, 2014). The PDSI is a standardized indicator with a range of 0 to +10 (dry to wet), with values below 3 indicating severe to extreme drought (Rimkus *et al.*, 2017).

The advantage of PDSI; The index's popularity and wide application in drought monitoring may be attributed to the fact that it provides decision makers with a measurement of the abnormality of recent weather for a region; an opportunity to place current conditions in historical perspective; and spatial and temporal representations of historical droughts (Agwata, 2014). The index is most effective measuring impacts sensitive to soil moisture conditions, such as agriculture; is useful as a drought monitoring tool and has been used to trigger actions associated with drought contingency plans.

Shortcomings of PDSI include: The lag between precipitation and runoff is not considered. Runoff is normally under estimated due to the model that only considers runoff once water capacity of surface and sub-surface soil is full; therefore, PDSI is ineffective in areas where runoff and precipitation are highly variable.

PDSI is less well-suited for mountainous land or areas of frequent climatic extremes; is complex and has an unspecified, built-in time scale that can be misleading (Agwata, 2014). Since the PI is sensitive to the AWC of a soil type, using it for a climate division might be too wide. The two soil layers used in water balance calculations are simplistic and may not be accurately indicative of a specific area (Sciences, 2012)

### **2.5.3 Standardized Water Supply Index (SWSI)**

The SWSI is a hydrological drought index that was developed to complement the PDSI in areas where local precipitation is not the primary source of stream flow in order to include snowpack also as a key element of water supply (Sciences, 2012). This index was designed to work best in mountainous areas with significant snowfall because of delayed contribution of snowmelt runoff to surface water supplies. It has the benefit of being simple to calculate and providing a representative measurement of surface water supply across a basin. One of the main limitations of the SWSI; It represents water supply conditions unique to a basin and has the disadvantage that changing a data collection station or water management requires that 13 new algorithms be calculated, and the index is unique to each basin, which limits inter basin comparisons (Agwata, 2014). That is to say, one cannot compare SWSI values between basins and regions.

### **2.5.4 Crop Moisture Index**

Palmer introduced Crop Moisture Index (CMI), a new drought index dependent on weekly mean temperature and precipitation, three years after introducing PDSI CMI measures moisture availability in major crop-producing regions over the short term and is not intended to determine long-term drought (Rimkus *et al.*, 2017).

Shortcomings of CMI: The index is not effective for long-term drought monitoring since it is designed for short term soil moisture demand of crops. CMI is not useful for crop initiation periods when it differs from place to place-seed germination.

### **2.5.5 Standardized Precipitation Index**

Tom McKee, Nolan Doesken, and John Kleist of the Colorado Climate Centre established the SPI in 1993 to measure the precipitation deficit over a variety of timescales and locations. The effect of drought on the availability of various water supplies is represented by these timescales, which include days, weeks, months, and years. 1-month, 3-month, 6-month, 9-month, 12-month, and 24-month cycles are widely used to measure the SPI. These timescales are suitable for monitoring various forms of drought and correspond to different drought impacts. The SPI can be calculated for any location that has a long-term precipitation data (Mlenga, Jordaan and Mandebvu, 2019). This long-term data is fitted to a probability distribution, which is then converted into a normal distribution to monitor dry and wet periods, resulting in a mean SPI of zero for the desired position and time (Mlenga, Jordaan and Mandebvu, 2019).

The SPI is globally the preferred index to be used for drought assessment because of its robustness and tractability (Abood and Mahmoud, 2018). Other benefits of the index include the fact that it can be computed for many time scales, can provide early warning of drought, can aid in drought severity assessment, and is simpler than the Palmer index (Agwata, 2014).

SPI is an appropriate index for drought study in East African countries, as indicated by many researches, when compared to other indices. For example, (Ntale, Gan and Mwale, 2003) said that SPI is better suited to monitoring droughts in East Africa because it is easily modified to the local climate, it requires less data, it generates spatially consistent results, and it can be computed almost at any time scale (Mekonen, Berlie and Ferede, 2020).

However, one of the SPI's flaws is that it does not include evapotranspiration in its equation. Since evapotranspiration is included in the mathematical equation, the Standard Precipitation Evapotranspiration Index (SPEI) is a stronger measure than the SPI. However, the availability of data is the most significant obstacle to the SPEI's implementation. Since evapotranspiration data for the entire district is not available for this study, the SPI was chosen as the indicator.

#### **Interpretation of SPI values.**

When the SPI is consistently negative and reaches an amplitude of -1.0 or less, a drought event occurs; the event stops when the SPI is positive, meaning that the negative values signify drought, while the positive values refer to wet conditions. Each drought event, therefore, has a duration

defined by its beginning and end, and intensity for each month that the event continues (Mlenga et al., 2019 and McKee et al., 1993) described drought intensities as a result of the SPI using the classification method.

**Table 1:Category of SPI based on range values (source:(Chopra, 2006)**

<b>SPI Range</b>	<b>Category</b>
2.0+	Extremely wet
1.5 to 1.99	Very wet
1.0 to 1.49	Moderately wet
-1.0 to -1.49	Near normal
-1.5 to -1.99	Moderately dry
-.99 to .99	Severely dry
-2 and less	Extremely dry

## **2.6 Satellite based drought indices for Agricultural drought characterization**

Remote sensing-based drought monitoring can be done using vegetation indices such as the Normalized Difference Vegetation Index (NDVI), Vegetation Condition Index (VCI), Temperature Condition Index (TCI). The NDVI and VCI are completely based on the vegetation, TCI takes into account the temperature factor (Belal *et al.*, 2014; Aswathi *et al.*, 2018). The agricultural drought monitoring in this study will be carried out using NDVI because, among all the vegetation indices available, it is a widely appropriate index for operational drought assessment due to its ease of measurement, interpretation, and ability to partially compensate for the effects of atmosphere, illumination geometry (Gupta et al., 2013).

### **2.6.1 Vegetation Condition Index (VCI)**

It was first suggested by Kogan (Thenkabail, Gamage and Smakhtin, 2004; Vogt *et al.*, 2018) VCI is an indicator of the status of the vegetation cover as a function of the status of the vegetation cover as a function of the NDVI minimum and maxima encountered for a given ecosystem. VCI is used to recognize drought situations and determine when they begin, especially in areas where drought episodes are localized and poorly defined. It focuses on the effects of drought on vegetation, and by noting vegetation changes and contrasting them to historical values, it can provide information on the onset, extent, and severity of drought.

Short coming of VCI: Potential for cloud contamination as well as a short period of record (Meteorological *et al.*, 1906).VCI has very low value in case of high cloud cover, thus wrongly depicting them as drought prone areas. To overcome such problems, the temperature-based indices can be used, which uses the thermal band derived brightness values to compute TCI (Aswathi *et al.*, 2018).

The combination of NDVI and LST provides very useful information for monitoring and assessing drought and developing an early warning system for drought especially to the farmers (Sruthi and Aslam, 2015).Unlike the meteorological based drought estimation, VCI provides satellite based near real time data with comparatively high spatial resolution (Quiring, 2009).

VCI compares the current NDVI to range of values observed in the same period in previous years. The vegetation condition index is expressed in percentages and gives an idea where the observed value is situated between the extreme values (minimum and maximum) in previous years. Lower and higher values indicate bad and good vegetation state conditions respectively. VCI varies from 0 for extremely unfavorable conditions to 100 for optimal. VCI is computed using the formula below;

$$VCI = \frac{NDVIa - NDVIMIN}{NDVIMAX - NDVIMIN} * 100$$

Where; NDVIa is the NDVI of the current month of observation.

NDVIMIN is the minimum NDVI value throughout the period of observation.

NDVIMAX is the maximum NDVI value throughout the period of observation.

VCI has been described as an accurate parameter for drought assessment but it is not enough to use it alone (Sholihah *et al.*, 2016). It is therefore better to combine the Vegetation Condition Index (VCI) with Land Surface Temperature (LST).

### **2.6.2 Temperature Condition Index (TCI)**

Temperature Condition Index (TCI) was also suggested by Kogan (1997). TCI is used to assess how temperatures and excessive wetness affect vegetation. The conditions are measured using maximum and minimum temperatures, and then updated to account for different vegetation responses to temperature (Svoboda and Fuchs, 2017). TCI is based on brightness temperature and measures the difference between the current month's temperature value and the maximum

temperature observed in the previous month (Chopra, 2006). Drought-affected areas can also be observed before biomass degradation occurs using meteorological measurements and the relationship between ground surface temperature and moisture regimes. As a result, TCI is crucial in drought monitoring. Shortcomings of Temperature Condition Index are potential for cloud contamination as well as a short period of record.

TCI identifies vegetation stress caused by high temperature, as well as excessive wetness and mostly used to observe changes in vegetation condition from bad to optimum (Singh, Roy and Kogan, 2003). Conditions are estimated relative to the maximum and minimum temperatures and modified to reflect different vegetation responses to temperature. TCI varies from 0 for extremely unfavorable conditions to 100 for optimal conditions. The TCI is obtained using the formula below;

$$TCI = \frac{LST_{max} - LST_a}{LST_{max} - LST_{min}} * 100$$

Where;  $LST_a$  is the temperature value of the current month.

$LST_{max}$  is the maximum temperature value throughout the observation period.

$LST_{min}$  is the minimum temperature value throughout the observation period

### 2.6.3 Normalized Difference Vegetation Index (NDVI)

Tucker first suggested NDVI in 1979 as an index of vegetation health and density (Hammouri and El-Naqa, 2007). NDVI has been extensively used for vegetation monitoring of wide areas, crop yield assessment, and drought detection (Himanshu, Singh and Kharola, 2015; Abood and Mahmoud, 2018). As a result, Vegetation is constantly monitored for conditions of drought using the Normalized Difference 16 Vegetation Index (Senay et al., 2014). The formula is used to calculate this index from a satellite image using spectral radiance in red and near infrared reflectance (Belal *et al.*, 2014);

$$NDVI = \frac{NIR - RED}{NIR + RED}$$

Where: NIR = The amount of near infrared light reflected by the vegetation and captured by the satellite sensor. RED = The amount of red light in the visible spectrum that is reflected by the vegetation and captured by the satellite sensor.



This is due to the fact that healthy vegetation absorbs the majority of visible light and reflects a significant portion of near-infrared light. Vegetation that is unhealthy or sparse reflects more visible light and less near-infrared light. In the red and infrared portions of the electromagnetic spectrum, bare soils, on the other hand, reflect moderately. Theoretically, NDVI is a nonlinear function that ranges between -1 and +1 (Hammouri and El-Naqa, 2007). However, in practice extreme negative values represent water, snow, ice and non-vegetated surfaces. Values around zero represent bare soil and values over 0.6 represent dense green vegetation, lower NDVI values are indicators of prevalence of drought condition (Belal *et al.*, 2014).

A variety of Studies have assessed drought using NDVI for example, Tucker and Choudhury (1987) found out that NDVI may be used as a response variable in semiarid and arid environments to identify and quantify drought disturbance, with low values indicating stressed vegetation. Based on the correlations between NDVI and a meteorologically based drought index, Ji and Peters (2003) discovered that NDVI is an efficient indication of vegetation response to drought in the Great Plains of the United States.

Limitations of NDVI; NDVI can be affected by cloud and cloud contamination, however, the maximum NDVI in a 10-day period (maximum NDVI composite) is used for a given pixel to minimize the impact of clouds (Senay *et al.*, 2014). NDVI uses only two bands and is not very sensitive to influences of soil background reflectance at low vegetation cover (Thenkabail, Gamage and Smakhtin, 2004).

In conclusion, it should be noted that various indices for different drought types are available as discussed and that different indices have strengths and weaknesses and not a single index is superior to the rest in all circumstances but some indices may be better suited than others for certain applications (Agwata, 2014).

The standardized precipitation index (SPI) will be considered as the superior index because it has several characteristics that are an upgrading over other indices, it is simple to calculate, has been widely used and it is recommended by many studies (Morid, Smakhtin and Moghaddasi, 2006). Additionally this index is less data intense therefore efficient for developing countries like Uganda where the access to data is limited (Mekonen, Berlie and Ferede, 2020) as it gives best result without other climatic parameters like minimum and maximum temperature, humidity, potential evapotranspiration and sun hours as it uses only precipitation data and gives accurate result (Shah,

Bharadiya and Manekar, 2015) and is able to characterize drought at different aggregate period, describing the dry and wet periods (Bayissa *et al.*, 2019). Sometimes it may be necessary to combine indices in a study to be able to comprehensively deal with the drought hazard. The indices should, however, not be based on identical data. The choice of an index depends on the purpose of a study and for drought risk assessment for instance, SPI is the most preferred index since it takes into account the component of precipitation deficit at different time scales and is generally used together with NDVI which is completely based on the vegetation and use of satellite data.

The Normalized Difference Vegetation Index (NDVI) is one of the most successful indices for simple and quick identification of vegetated areas and their condition (Agone and Bhamare, 2008). The NDVI from LANDSAT 8 LOI data has been extensively used for vegetation monitoring, crop yield assessment, and drought detection (Bera *et al.*, 2018). Thus, these methods are better for agricultural (vegetation stress) and Meteorological (precipitation) drought applications and henceforth for this study.

#### **2.6.4 Vegetation Health Index**

The Vegetation Health Index (VHI) combines VCI and TCI. The VHI is based on vegetative data collected for a long term sequence basically extracted from remote sensing data thus it can be noticed that the ratio of LST/NDVI increases during times of drought. The vegetation health index averages the sum of Vegetation Condition Index and Temperature Condition Index. The VHI has also been frequently used for agricultural purposes, such as crop yield estimation [Kogan *et al.*, 2012, Salazar *et al.*, 2008, Bokusheva *et al.*, 2016]. The principle of using VHI for drought monitoring is that an assessment of temperature conditions helps identify subtle changes in vegetation health because the effect of drought is more drastic if shortage of moisture is accompanied by excessive temperatures. The feasibility of using VHI has been validated in all major agricultural countries. The VHI is computed using the formula below;

$$\mathbf{VHI = \alpha VCI + (1-\alpha) TCI}$$

where  $\alpha=0.5$  (Sholihah *et al.*, 2016)

The VHI range developed by (Kogan, 2002) are shown in the table below;

**Table 2: Category of VHI based on range values (source: (Kogan, 2002))**

Drought classes	VHI
Extreme drought	<10
Severe drought	10-20
Moderate drought	20-30
Mild drought	30-40
No drought	>40

## 2.7 Land Surface Temperature (LST)

Land surface temperature is derived from the thermal infrared bands of satellite images. It serves as a proxy for assessing evapotranspiration, vegetation water stress and soil moisture (Karnieli *et al.*, 2010). LST is a good indicator of the energy balance at the earth's surface which can provide important information about the surface physical properties and climate (Goetz, 1997; Sruthi and Aslam, 2015). It is reported that the negative correlation between LST and NDVI was largely due to changes in vegetation cover and soil moisture and indicated that the surface temperature can rise rapidly with water stress.

### 2.7 LST estimation

#### 2.7.1 The Qin et al.'s mono-window algorithm

The mono window algorithm estimates LST through decomposition of Planck's radiance function using a Taylor's expansion and calculation of two empirical coefficients a and b (Qin et al., 2001). Three a priori known parameters are required for the algorithm: transmissivity ( $\tau$ )/water vapour content, effective mean atmospheric temperature ( $T_a$ ) and emissivity ( $\epsilon$ ). All the temperatures are in Kelvin. LST ( $T_s$ ) is calculated from the equation below;

$$T_s = \{a(1 - C - D) + [b(1 - C - D) + C + D] \times T_{sensor} - DT_a\} / C$$

Where  $a = -67.355351$  and  $b = 0.458606$  are constants,  $T_{sensor}$  is the at-sensor brightness temperature,  $T_a$  can be calculated from the total water vapor content and the near surface local air

temperature depending on the atmospheric conditions, C and D are calculated using the equations below respectively;

$$C = \varepsilon\tau$$

$$D = (1 - \tau) [1 + (1 - \varepsilon)\tau]$$

The main disadvantage of this method is that it is dependent on water vapor and other atmospheric conditions and requires in-situ measurements.

### 2.7.2 Single channel algorithm

The recent Single channel modification is highly sensitive to water vapor changes (Cristóbal *et al.*, 2009). Therefore, it means that in absence of the in situ measurements of water vapor content this method cannot be used to estimate LST. Since LST estimation methods require clear sky, only cloud-free images are used for processing. In this method LST is obtained from the following equation;

$$T_s = \gamma \left[ \frac{1}{\varepsilon} (\psi_1 L_{sensor} + \psi_2) + \psi_3 \right] + \delta$$

Where:  $\varepsilon$  is surface emissivity,  $\gamma$  and  $\delta$  are parameters directly depending on Planck's function. Also  $\psi_1$ ,  $\psi_2$  and  $\psi_3$  are the atmospheric correction functions. Similar to the MW, the optimal performance of the SC algorithm is observed for the atmospheres with water vapor content in the range of 0.5–2.5 g·cm<sup>-2</sup> (Qin *et al.*, 2001).

### 2.7.3 Radiative transfer equation

This equation is used to estimate the land surface temperature from the thermal infrared region of the spectrum. It depends on the wavelength but also on the observation angle, although for Landsat, the nadir view provides good results. The atmospheric parameters are calculated from in situ radio soundings and using a radiative transfer codes like MODTRAN (Jimenez-Munoz *et al.*, 2009).

$$L_{\text{sensor},\lambda} = \left[ \varepsilon_{\lambda} B_{\lambda}(T_s) + (1 - \varepsilon_{\lambda}) L_{\text{atm},\lambda}^{\downarrow} \right] \tau_{\lambda} + L_{\text{atm},\lambda}^{\uparrow}$$

where  $L_{\text{sensor}}$  is the at-sensor radiance or Top of Atmospheric (TOA) radiance (the radiance measured by the sensor),  $\varepsilon$  is the land surface emissivity,  $B_{\lambda}$  is the blackbody radiance given by the Planck's law and  $T_s$  is the LST,  $L_{\text{atm},\lambda}^{\downarrow}$  is the down welling atmospheric radiance,  $\tau$  is the total atmospheric transmissivity between the surface and the sensor and  $L_{\text{atm},\lambda}^{\uparrow}$  is the upwelling atmospheric radiance. Therefore, from Equation above it is possible to find LST by inversion of the Planck's law. The main disadvantage of this method is that it needs in situ Radio sounding launched simultaneously while the satellite passes.

## 2.8 The methods used in previous studies

Many studies have been done on drought forecasting adopting different indices and prediction models especially with the advent of remote sensing technology. These variations have occurred mainly due to a difference in the accuracies and efficiency of various indices and prediction models. Satellite remote sensors can quantify what fraction of the photo synthetically active radiation is absorbed by vegetation (Ghobadi *et al.*, 2015). A region's absorption and reflection of photo synthetically active radiation over a given period of time can be used to characterize the health of the vegetation there, relative to the norm with the calculation of NDVI for the region.

(Sruthi and Aslam, 2015) Combined EROS Moderate Resolution Imaging Spectroradiometer (eMODIS) NDVI data and MOD11A2 LST data extracted from MODIS for drought assessment. NDVI and quality data were used to calculate the NDVI metrics. eMODIS NDVI data values range from -1999 to 10000, 2000 being the fill value. After applying the scale factor, the NDVI data values were found to lie within 0 to 1. Time-series NDVI variation profile of the study area was derived from the calculation of NDVI using the eMODIS NDVI data for the specified period of time and also used to generate the maximum, minimum and average NDVI values of every month. Land Surface Temperature was calculated from the MOD11A2 data but extracted in Kelvin. The digital number (DN) values were converted to degrees Celsius using the formula below; Temperature = (DN \* 0.02) - 273.15 °c

The monthly average temperature of the study area was calculated and the values correlated with the monthly NDVI values in order to understand the changes in vegetation growth with respect to the rainfall and temperature, thereby indicating the intensity of agricultural drought.

(Karthika, et al., 2017) Used the first step of the ARIMA model to get the Vegetation Temperature Condition Index (VTCI) image of the first ten days of April in 2006 for the Guanzhong Plain in China. Step 2 of the ARIMA model was then used to forecast the VTCI image of the middle ten days of April for the same year. By comparing the original data with the predicted ones, the two images were found to be similar hence the conclusion that the model was accurate and suitable for drought prediction in China.

(Dutta *et al.*, 2015) Combined a Vegetation Condition Index (VCI) and Standardized Precipitation Index (SPI) for drought assessment in the North Western part of India. The Vegetation Condition Index was computed using the formula stated earlier in this report. The VCI were classified according to drought severity classes developed by (Singh et al., 2003). The Standardized Precipitation Index (SPI) was computed using the formula below;

$$SPI = (x^{\alpha-1} \cdot e^{-x/\beta}) / (\beta^\alpha \cdot \Gamma(\alpha))$$

Where  $\alpha > 0$ , is a shape parameter,  $\beta > 0$  is a scale parameter,  $x$  is the precipitation amount and  $\Gamma(\alpha)$  is the gamma function.

A Crop Yield Anomaly was then computed for identifying deviation of yield for a particular from its long term period basically giving the statistics of major rain fed crops like maize, sorghum and Pearl millet. Yield anomalies of these crops were calculated using the formula below;

$$YAI = (Y - \mu) / \delta$$

Where, YAI = Yield Anomaly Index

Y = Crop Yield

$\mu$  = Long term average yield

$\delta$  = Standard Deviation.

It was discovered that unlike the meteorological data available from sparsely distributed meteorological stations, remote sensing based index VCI can be successfully used for delineating the spatio-temporal extent of agricultural drought (Dutta *et al.*, 2015).

(Sun and Kafatos, 2007) Used the period between 1996-2000 because improved information on clear sky radiances and cloud cover was available. Clear sky conditions were selected to calculate skin temperature (LST) for cases where the cloud cover fraction (CCF) was less than 10%. To test for the quantitative relations from daily maximum, minimum and mean LST, the following equation was used;

$$LST_{max}/LST_{min}/LST_{mean} = a + bNDVI$$

Where a and b are the regression coefficients. Correlation analysis' were performed with monthly mean values of spatial points from the five-year average of North America. The correlations between NDVI and surface air temperature were generally positive in winter period, negative in summer and insignificant in autumn.

(Van Rooy,1965) Developed the “Rainfall Anomaly Index” (RAI) based on ratios of rainfall departure from normal to departure of threshold value from normal. It is dependent on long term meteorological rainfall observations. RAI shows the relation between a regional humidity index and the actual evaluation of dry periods during the rainy season. The demerit of this index is that it uses the observations from only rainfall.( Alley,1984)Stated that the “Palmer Drought Severity Index” (PDSI) was developed for Meteorological drought assessment using precipitation, evapotranspiration and soil moisture conditions as the key inputs. The PDSI is efficient in addressing two of the most significant properties of drought and they are the intensity of drought and its onset and offset time. However, PDSI is very complicated to compute and requires a long term observations of multiple parameters which makes it usable at only limited regions. It has some other limitations too due to which, the conventional time series models may not be able to capture the stochastic properties of PDSI.

(Tsakiris and Vangelis, 2005) Used the “Reconnaissance Drought Index (RDI)” for assessment of drought severity. Here, the Potential Evapotranspiration (PET) is calculated using Thornthwaithe formula. Rainfall and temperature data are obtained for monthly time steps. Since PET is used, a realistic determination of water deficit is obtained.

(Karthika, et al., 2017) Used the ARIMA model to predict rainfall data in the semi-arid region of India and made a comparison between the observed data and predicted data with the purpose of

validating the model. It was discovered that the predicted data arguably agreed with the actual data (Karthika, et al., 2017). According to research, combining vegetation indices with an appropriate prediction model gives a good basis for making drought prediction or future rainfall patterns.

## **2.9 Digital image processing**

The main goal of digital image processing is to improve the quality of tones and hues, image textures, fracture patterns, lineaments, and their trends in order to increase the amount of geological information extracted (Lineament *et al.*, 2012). Digital image processing is categorized into:

- (i) pre-processing techniques for example geometric and radiometric corrections of the satellite raw data, mosaicking and sub setting techniques for the targeted area
- (ii) Image enhancement techniques are methods for creating new updated images with more detail in order to make visual representations of specific features easier. Digital image processing is ended by the information extraction procedures including image classification techniques (Lineament *et al.*, 2012).

### **2.9.1 Image pre-processing**

Pre-processing functions involves the operations required prior to the main data analysis and consists of processes aimed at geometric correction, radiometric correction and atmospheric corrections present in the raw image data to improve the ability to interpret the image components qualitatively and quantitatively. This process corrects the data for sensor irregularities and removes (radiometric corrections) unwanted sensor distortion or atmospheric noise (Asokan *et al.*, 2020). Sensor, solar, atmospheric, and topography influences can cause distortion in images obtained by Landsat sensors. Preprocessing attempts to minimize these effects to the extent desired for a particular application (Young et al., 2017).

### **2.9.2 Radiometric and Geometric correction**

Satellite images are normally subjected to radiometric and Geometric correction in order to correct for some of the errors in the image.

#### **2.9.2.1 Geometric correction**

It entails correcting geometric distortions caused by sensor-Earth geometry variations as well as converting data to real-world coordinates (Geo- Referencing). Geometric errors are present in image data captured by satellite sensors. The relative movements of the platform, its scanners, and



the earth trigger an image geometry error. Geometric errors of varying degrees can be caused by non-idealities in the sensors, the curvature of the earth, and uncontrolled changes in the location and altitude of the remote sensing platform (Asokan *et al.*, 2020).

#### ***2.9.2.2 Radiometric correction***

A sensor detects reflected electro-magnetic energy; however, due to the sun's azimuth and atmospheric conditions, the detected energy differs from the energy emitted by the same source. As a result, these radiometric distortions must be corrected in order to achieve the true irradiance or reflectance. Radiometric correction plays a critical role in producing an error-free thematic map for biomass applications. To correct radiometry for terrain topography and canopy variations due to reflectivity, Simard *et al.*, (2016) suggested holomorphic and heteromorphic calibration technique.

### CHAPTER THREE: METHODOLOGY

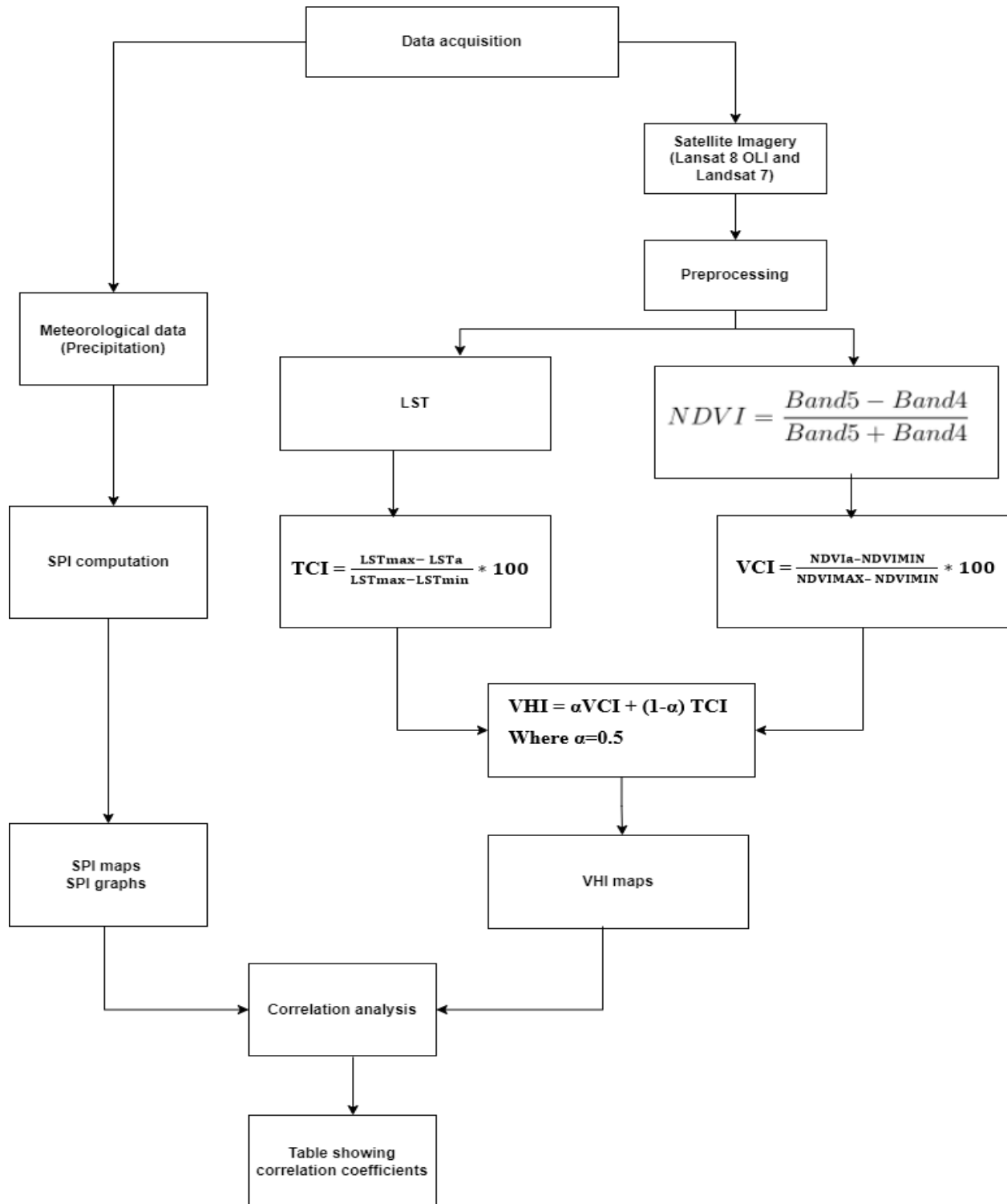


*Figure 2: Shows the methodology flow chart*

### **3.1 Data collection**

The first phase of the methodology was data acquisition. Data was acquired from satellite sources and meteorological datasets were obtained from the Uganda National Meteorological Authority and the global weather database Soil and Water Assessment Tool. The satellite imagery for this study were obtained for Landsat 8 OLI with a spatial resolution of 30m for January 2015,2020 and Landsat 7 ETM for 2000,2005,2010 were downloaded from USGS (United States Geological Survey) with a 5 years' interval. Landsat's resolution has the implication that it is not flooded with microscopic detail but incorporates features that are sufficient for identification of built-up and non-built-up enabling classification (Taubenboeck et al., 2008). In January there is not any or very little rainfall (the rainy season usually stretches from March to May and later from August to November) when the ecosystem-based adaptations to drought are assumed to be at their peak. January falls in the dry season hence a higher chance of clear imagery without cloud cover being a problem. Therefore, all the images were acquired for the month of January.

The study area is one of Uganda's less well-monitored areas in terms of the dense meteorological data collection networks. The existing meteorological datasets have a series of gaps and cannot be filled and used for drought assessment (Mfitumukiza et al., 2017). The gaps are attributed to vandalism and subsequent system breakdowns. Due to this shortcoming, this study downloaded and used some of the meteorological datasets from the global weather database Soil and Water Assessment Tool (<http://globalweather.tamu.edu/>). These datasets have been used to assess droughts in the East African region (Mfitumukiza et al., 2017). The defined period of data collection was from 01/01/2000 to 31/12/2020 from the Uganda National Meteorological Authority.

### **3.2 Data processing**

#### **3.2.1 Image pre-processing**

Already processed and cloud cover free Landsat 8 and 7 imagery of collection 2 level-1 were downloaded from USGS (United States Geological Survey) with a 5 years' interval. The corrections were carried out on Landsat 7 ETM+ and Landsat 5 imagery to remove strip lines. These were corrected using QGIS software where rasters were imported and then spatially corrected for a number of times.

### 3.2.2 Clipping and masking to study area

The study area which is Isingiro district was clipped out in ArcGIS software using the administrative boundary shape files of districts in Uganda that were obtained from the UBOS website for efficient processing. The same shape file was used as the mask for extracting images for classification. The extract by mask tool in ArcGIS software was used. This resulted into the shape files and imagery covering only the study area.

### 3.3 Computation of Normalized Difference Vegetation Index (NDVI)

Normalized Difference Vegetation Indices for the years 2000-2020 were calculated based on Landsat 8 and 7 satellite images in ArcGIS software. NDVI calculation was performed to extract vegetation index values which were used for computing Vegetation Condition Index. For this study, NDVI was calculated for each of the five years according to the following formula; While using Landsat 8 image NDVI was calculated using;

$$NDVI = \frac{Band5 - Band4}{Band5 + Band4}$$

### 3.4 Computation of Vegetation Condition Index (VCI)

The Vegetation Condition Index was obtained from Normalized Difference Vegetation Index (NDVI) to monitor vegetation condition. The VCI data were derived using the following equation;

$$VCI = \frac{NDVIa - NDVIMIN}{NDVIMAX - NDVIMIN} * 100$$

### 3.5 Computation of Land Surface Temperature

The Digital Numbers (DN) were converted to physical measurements at sensor radiance ( $L_{\mu}$ ) using the formula below that accounts for the transformation function used to convert the analogue signal received at the sensor to DN stored in the resulting image pixels;

$$L_{\mu} = (\text{gain} * \text{DN}) + \text{offset}$$

Where  $L_{\mu}$  is at sensor radiance, gain is the slope of the radiance/ DN conversion function, DN is the digital number of a given pixel and offset is the intercept of the radiance/ DN conversion function. Gain and offset values were supplied in the metadata accompanying the image. The band

was then converted from spectral radiance to a physically useful variable using the formula below;

$$TB = K2 / (\ln (K1 / L\mu + 1))$$

Where TB is the radiant surface temperature (K), K2 is the calibration constant 2 (1282.71), K1 is the calibration constant 1 (666.09), and  $L\mu$  is the spectral radiance of thermal band pixels (YUE, et al., 2017).

Finally, the radiant surface temperature will be converted to Land Surface temperature (LST) using the formula;

$$LST = TB / (1 + \mu TB / \rho) \ln \varepsilon$$

Where  $\mu$  is the wavelength of emitted radiance (for which the peak response and the average of the limiting wavelengths ( $\mu=511.5$ ) were used),  $\rho = h * c/\alpha$  ( $1.438*10^22mK$ ),  $\alpha$  is Boltzmann's constant ( $1.38*10^{-23}J/K$ ),  $h$  is Planck's constant ( $6.626*10^{-34}Js$ ), and  $c$  is the velocity of light ( $2.998*10^8m/s$ ).  $\varepsilon$  is emissivity.

### 3.6 Computation of Temperature Condition Index (TCI)

The Temperature Condition Index was calculated using the following equation;

$$TCI = \frac{LST_{max} - LST_a}{LST_{max} - LST_{min}} * 100$$

Where,  $LST_a$  is the LST value of current month,  $LST_{min}$  and  $LST_{max}$  denotes the minimum and maximum LST values respectively calculated from multiyear time series data.

### 3.7 Computation of Vegetation Health Index

The VHI was computed using the Vegetation Condition Index (VCI) and the Temperature Condition Index (TCI) values. The vegetation health index was computed using the formula;

$$VHI = \alpha VCI + (1 - \alpha) TCI \text{ Where } \alpha = 0.5 \text{ (Shiddiq, et al., 2016)}$$

The periodic VHI values were plotted in Microsoft Excel to obtain a graphical trend of the past years. The VHI values were then classified basing on the drought severity classes developed by (Kogan, 2002) (*Table 2.2*)

### 3.8 Computation of Standardized Precipitation Index (SPI)

The Standardized Precipitation Index values were calculated according to the methodology explained by (Giddings et al., 2005). The SPI computations were achieved through the use of DrinC

software. Other studies according to (Mlenga et al.,2019 and Mondol et al., 2017) considered Drought Index Calculator (DrinC) software. Therefore, computing SPI was done by using the Drought Index Calculator (DrinC) which was developed by the Laboratory of Reclamation Works & Water Resources Management, National Technical University of Athens. The software was downloaded from [http:// www.ewra.net/drinc](http://www.ewra.net/drinc). The selection of the software was based on its simplicity such that it can be easily adopted for use. DrinC is a user-friendly tool software package that was developed for providing a simple and an adaptable interface for the calculation of several drought indices (Tigkas, Vangelis & Tsakiris 2015). The software operates on Windows platform and is programmed in Visual Basic. A series of 30 years (1990-2020) period of data was used to determine SPI values for 3-, 6- and 12-month timescales. The SPI was computed for on a monthly scale so that the consistency of drought condition and duration was determined according to SPI categories (table 1) that is to say, this allows establishing classification values for SPI. A series of 30 years (1990-2020) period of data was used to determine SPI values and the selected timescales for the computation of SPI were 3, 6 and 12-month time scales. The 3-month SPI indicates the conditions of short-term drought, mostly soil moisture and drought stress with an impact on agriculture, while the 6- and 12-month SPIs indicate medium to long-term droughts which affect ground water supplies and pasture conditions (Mlenga et al., 2019).

Isingiro district precipitation(rainfall) dataset for a period of thirty years (1990-2020) was obtained from Uganda National Meteorological Authority. The Microsoft Excel data set was uploaded onto the DrinC software for manipulation.

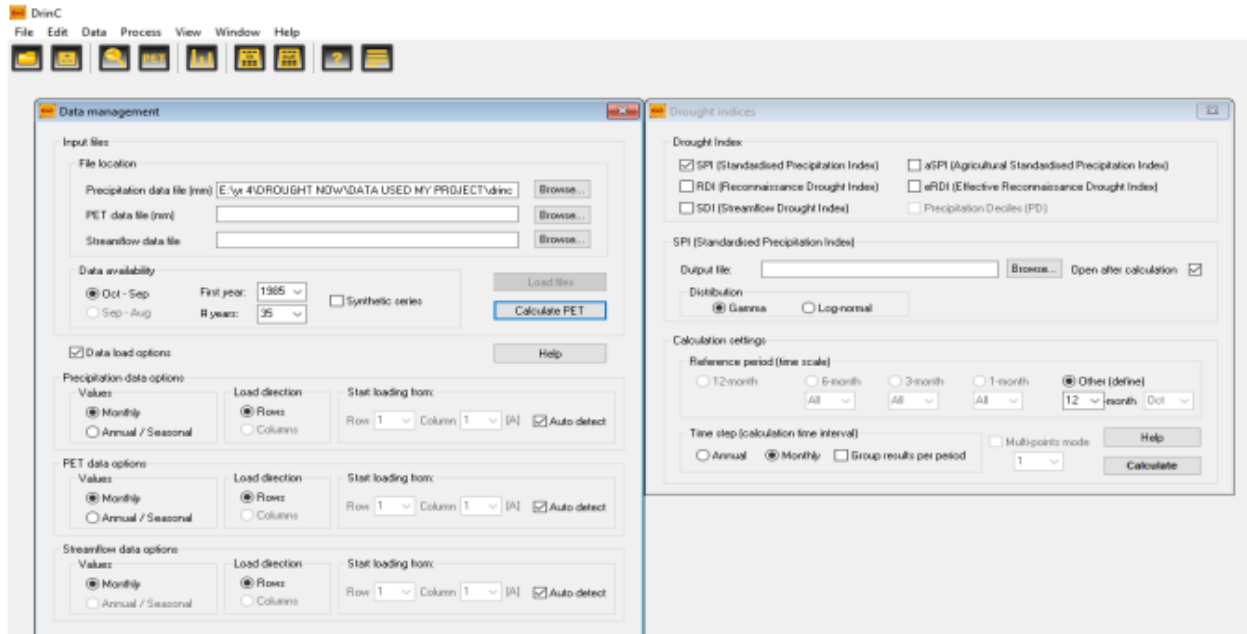


*Figure 3: Interface of DrinC software*

The SPI was calculated at 3-, 6- and 12-month timescales. The primary reference base in DrinC software is the hydrological year (October–September). However, the study defined the hydrological year based on the rainfall calendar of Isingiro district. The MS excel worksheet format output was produced and used for further processing in ArcGIS.

### **3.9 Generation of maps from SPI and VHI data**

Mapping is an essential part of the illustration of spatial drought as a visual and effective tool to compare and depict how drought is distributed in a region (Edwards, 2015). The SPI values were interpolated using Inverse Distance Weighted (IDW) method in ArcGIS software and the maps were generated for the years 2000, 2005, 2010, 2015 and 2020 for the 6-month SPI time scale. The interpolated maps were reclassified based on the SPI values as categorized in Table 1. Using the VHI values calculated, VHI maps were generated for the years 2000, 2005, 2010, 2015 and 2020.

## CHAPTER FOUR: RESULTS AND DISCUSSIONS

### 4.1 Introduction

This chapter presents, analyzes and discusses results obtained from analysis of Standardized Precipitation Index(SPI) and Vegetation Health Index in order to achieve the overall and specific objectives of this study. The results from assessment of objective one are presented first followed by those for objective two.

### 4.2 Results and Discussion

#### 4.2.1 Drought Severity and frequency

The utilization of Standardized Precipitation Index in quantifying various drought types is widely known. Because SPI may be estimated across a variety of time scales, it is frequently used as a drought indicator. The selected timescales for the computation of SPI were a 3,6 and 12-month for over 30years. SPI during selected years of 2000, 2005, 2010, 2015 and 2020 have been presented to show the pattern of SPI during these years.

##### 4.2.1.1 Standardized Precipitation Index (SPI) graphs

The plot shows both wet and dry years during the entire study period. Summaries of these graphs are shown below;

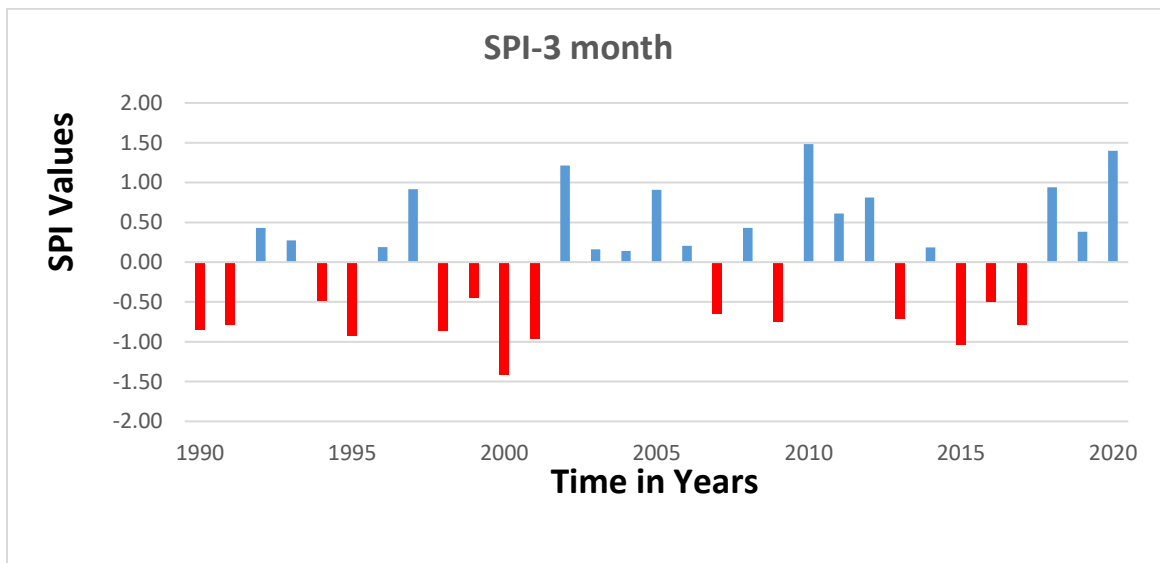


*Figure 4:SPI results at 3-month time scale*

From the figure above, Drought conditions result in a negative score while wet conditions result in a positive index. It is observed that rainfall variability is high shown by annual fluctuations



above and below the established zero causing wet and dry conditions. The index grows more negative or positive when the dry or rainy circumstances become more severe. Mfitumukiza et al. (2017) found that such weather extremes and climate events occur frequently in Uganda. According to the SPI statistics, the extreme drought years were 1990,1991, 1994, 1995,1998, 2000,2001, 2007, 2009,2015,2016 and 2017 for the assessed period, while the wettest years recorded included 2002, 2005, 2010, 2018, 2020.

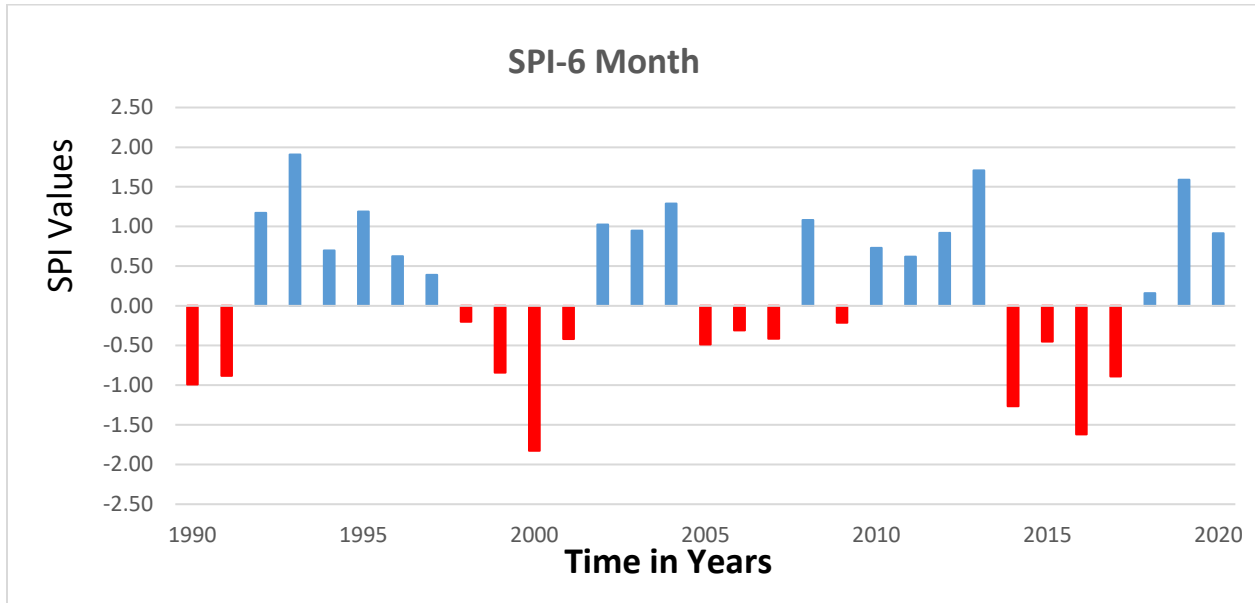


**Figure 5:SPI results at 6-month time scale**

The plot shows wet and dry (drought) years. The figure shows 1992,1993,1995,2004,2008, 2013, and 2019 as wet years and 1993,2013 and 2019 as the wettest years. On the other hand, the plot shows that the area experienced moderately and severe droughts between, (1990-1991) and later between 1999-2000 and 2014-2017. The plot also reports short-term normal droughts in 1998, 2005 -2007 and 2009.

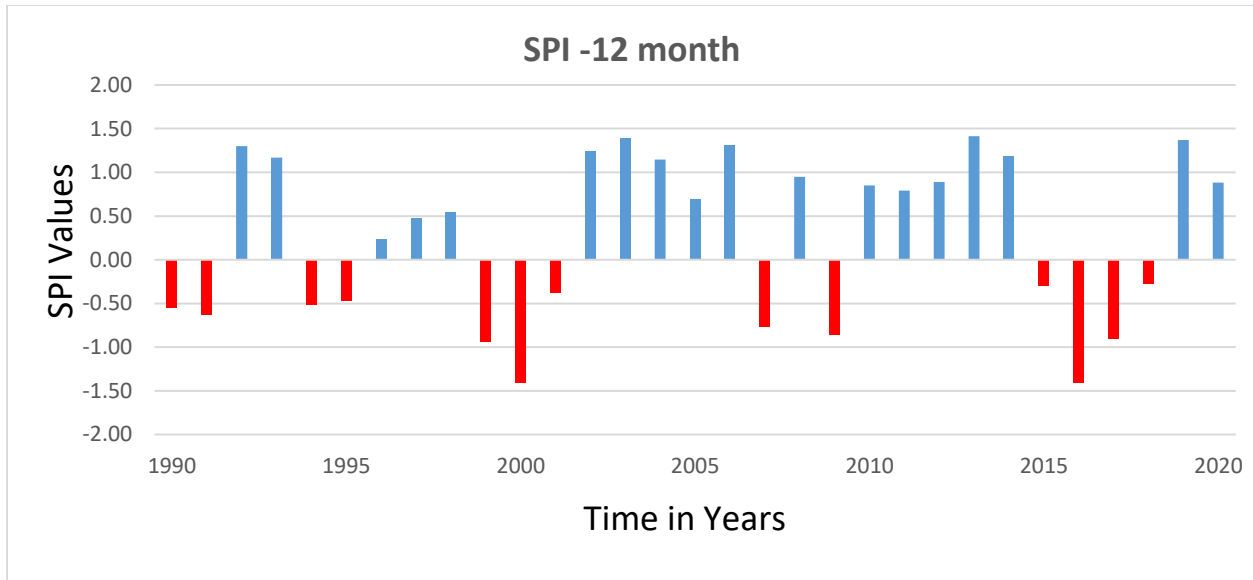


**Figure 6: SPI results at 12-month time scale**

The results above show that 2002-2006 and 2010-2014 were wet years. The plot also depicts droughts from 1999-2001 and from 2015-2018 with extreme droughts.

**4.2.1.2 Discussion**

For the period 1990-2020, the analysis demonstrates the temporal behavior of dry and wet conditions on a 3, 6, and 12-month time scales for Isingiro district for a period of 30 years. As indicated in table 1, the SPI values are separated into groups ranging from extreme wet to extreme drought. SPI-12-time scale had larger frequencies of change between the dry and wet periods but in SPI-6 and SPI-3 time scales it was medium. On a short timescale (SPI-3 and SPI-6 time scales) the fluctuation of the intensities was between less than -1 and less than 1 and the drought conditions were ranging from moderate to severe droughts. Droughts are constant in the periods 1998 to 2001 and 2015 to 2018 as indicated by the SPI-12-month scale. The highest SPI value for the 12-month scale (SPI-12) is -1.48 in 2017 and -1.46 for 2000. These high values were because of severe droughts experienced in that period. Two long-term droughts from 1998 to 2001 and 2015 to 2018 were recorded. This implies a considerable impact on reservoir levels and groundwater levels.

#### 4.2.2 Standardized Precipitation Index (SPI) drought maps

The SPI data values for the years 2000,2005,2010, 2015 and 2020 were analyzed to show the spatial pattern during these years. The calculated SPI values were interpolated using Inverse Distance Weighted method to identify drought prone areas in Isingiro district.

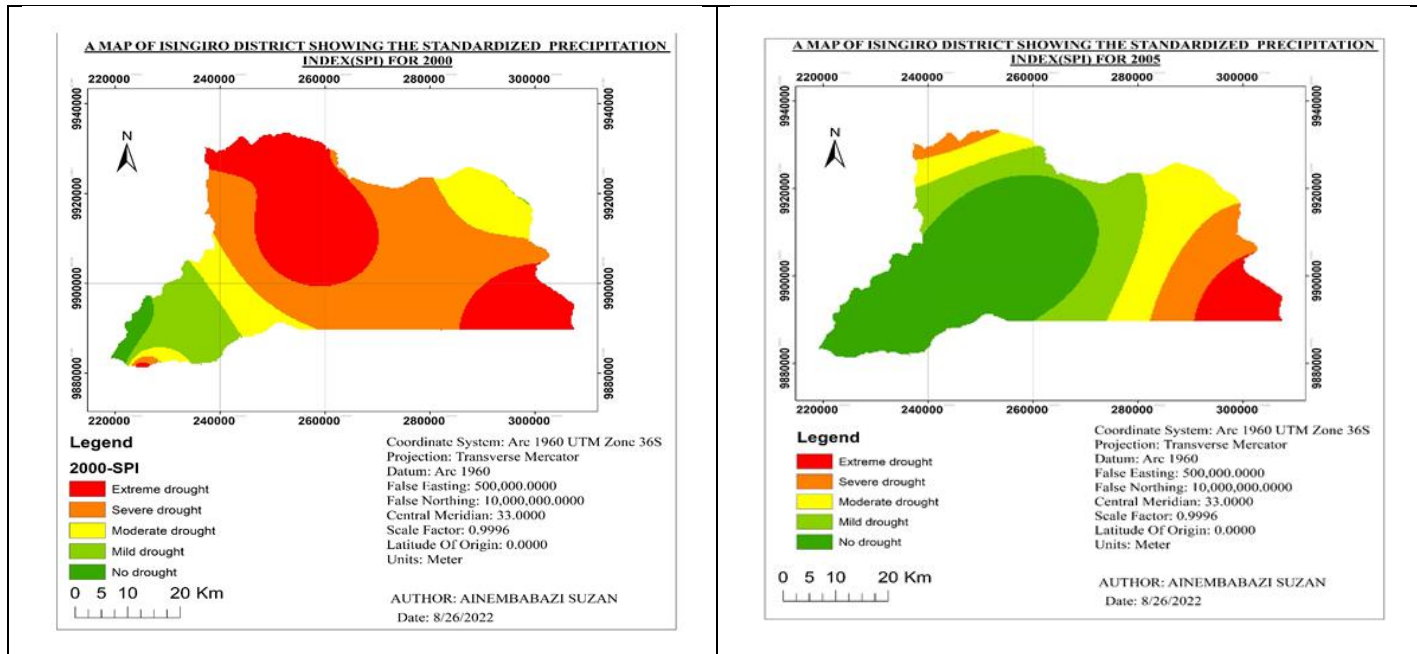


Figure 7: SPI maps of Isingiro district for the years 2000 and 2005

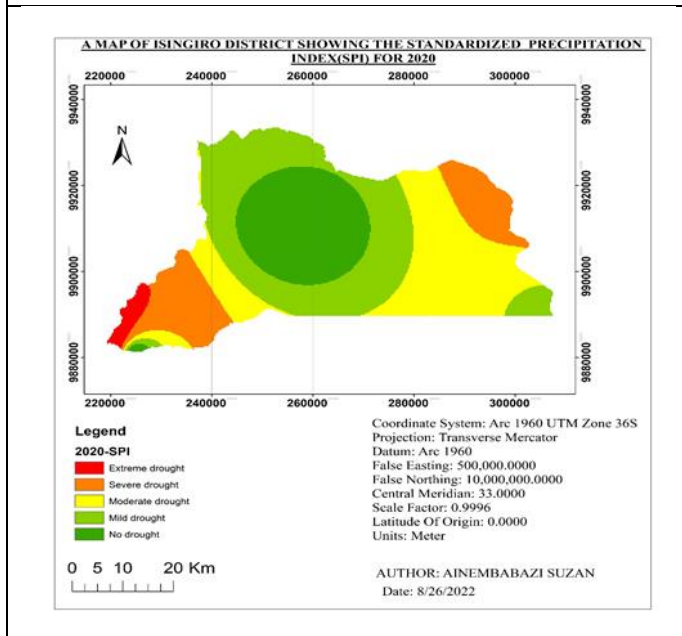
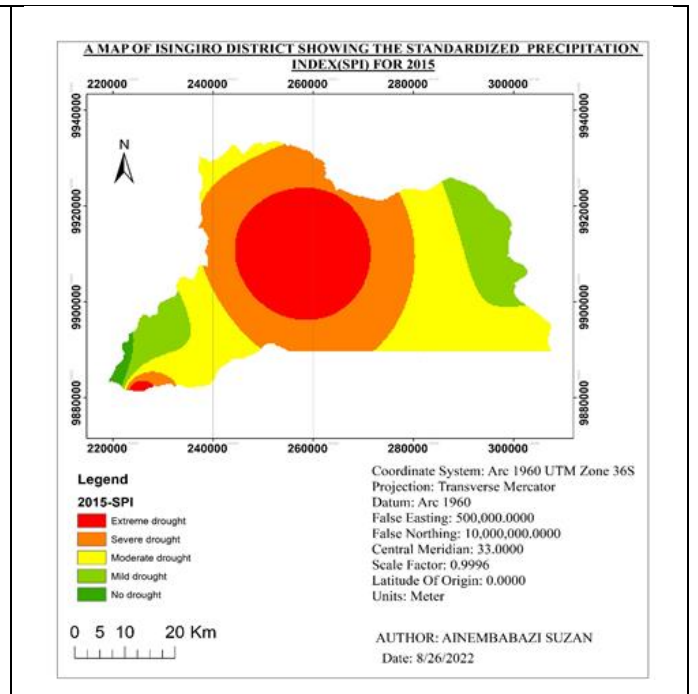
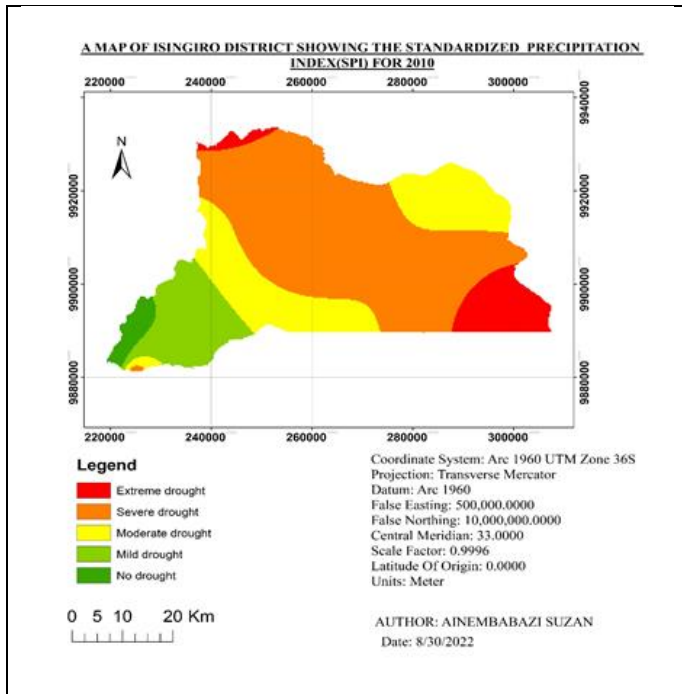


Figure 8: SPI maps of Isingiro district for the years 2010,2015 and 2020

#### ***4.2.2.1 Discussion***

The results indicate lower SPI values for the years 2000 and 2015 in the northern part and central part of Isingiro district. Isingiro district did not experience drought in the years 2005 and 2010 as seen from the maps, the SPI values were in the range of 1.0 to 1.5. In 2015 the SPI values dropped from 0.03 to -0.15 which indicates a severely dry situation and this was because of low precipitation received. In 2020 the SPI values were high between 0.43 and 1.85 in the western and central area of Isingiro district which indicate moderate and mild drought due to increased amount of rainfall received in 2019 and 2020. This variation helped in identifying the trend and the years in which the area was more prone to drought conditions due to precipitation.

### 4.2.3 Vegetation Health Index (VHI) drought maps

The VHI data values for the years 2000, 2005, 2010, 2015 and 2020 were analyzed to show the spatial pattern during these years.

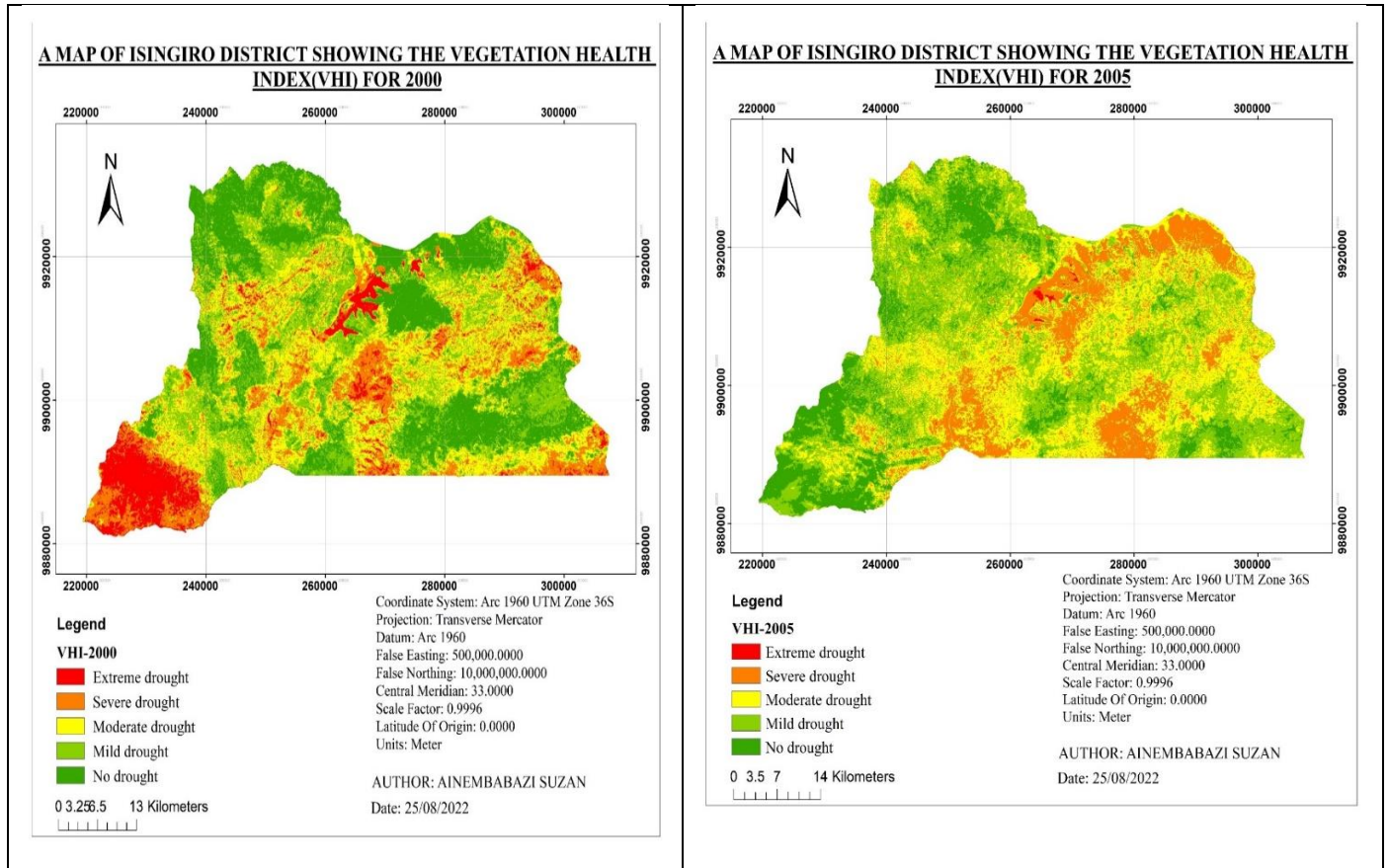


Figure 9: VHI maps of Isingiro district for the years 2000 and 2005

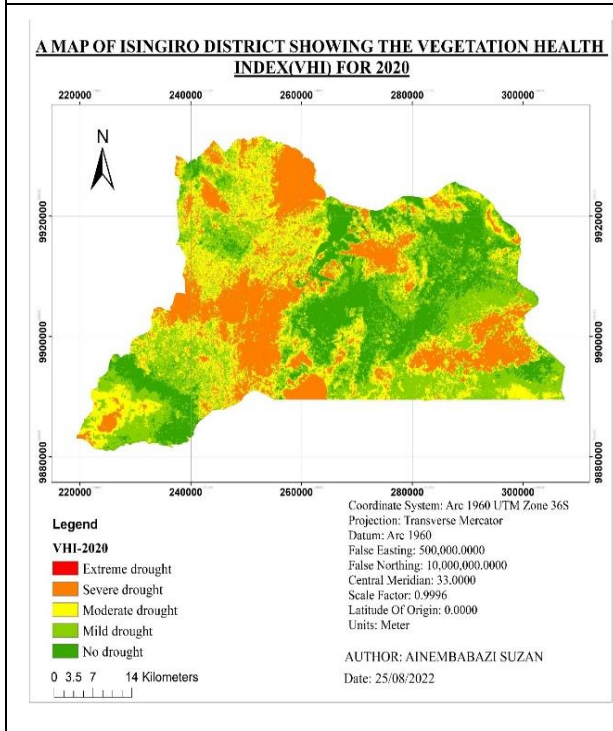
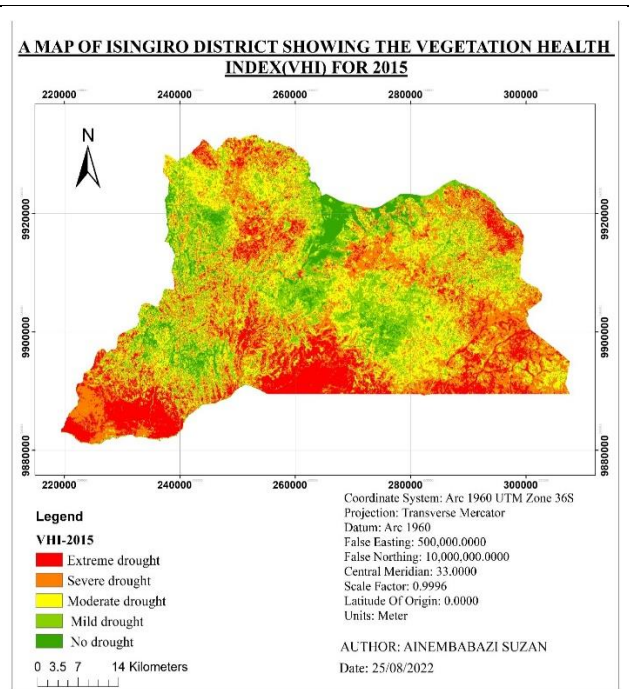
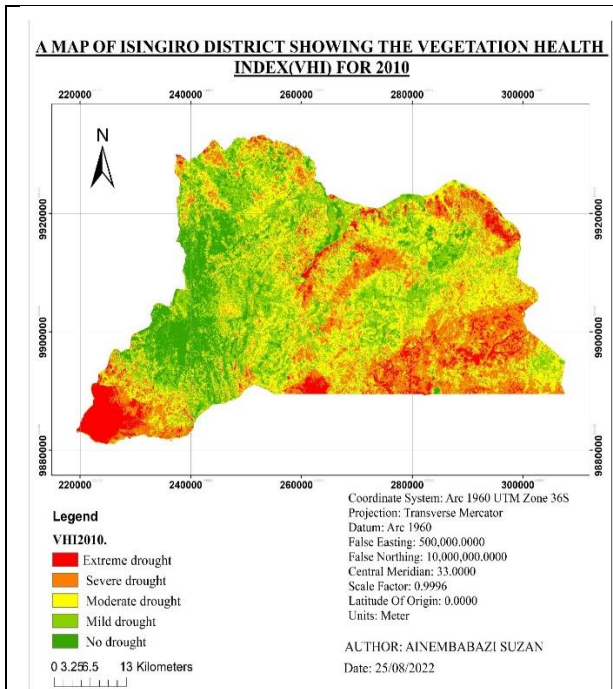


Figure 10: VHI maps of Isingiro district for the years 2010, 2015 and 2020



#### 4.2.3.1 Discussion

The drought maps were classified into five classes namely; No drought, Mild drought, Moderate drought, severe drought and extreme drought. The maps show the areas that were affected by in the years 2000, 2005, 2010, 2015 and 2020. These maps clearly give a scenario of drought prevalence and its trend in the area. In 2000, 2010 and 2015 drought was higher in extent than in 2005 and 2020. Therefore more focus has to be given to these areas when drought management plans are prepared. The tables below show the area and percentage for each class for the two different indices used to monitor drought.

**Table 3: Area and Percentage area of drought for the years 2000, 2005, 2010, 2015 and 2020 for SPI**

SPI	2000		2005		2010		2015		2020	
	Area in Sq.km	Area(%)	Area in Sq.km	Area(%)	Area in Sq.km	Area(%)	Area in Sq.km	Area(%)	Area in Sq.km	Area(%)
Extreme drought	933.35	31	301.08	10	541.95	18	662.38	22	331.19	11
Severe drought	1083.89	36	541.95	18	903.24	30	782.81	26	481.73	16
Moderate drought	572.05	19	451.62	15	632.27	21	903.24	30	692.49	23
Mild drought	301.08	10	602.16	20	331.19	11	541.95	18	843.03	28
No drought	120.43	4	1114.00	37	602.16	20	120.43	4	662.38	22
<b>Total</b>	<b>3010.81</b>	<b>100</b>	<b>3010.81</b>	<b>100</b>	<b>3010.81</b>	<b>100</b>	<b>3010.81</b>	<b>100</b>	<b>3010.81</b>	<b>100</b>

**Table 4: Area and Percentage area of drought for the years 2000, 2005, 2010, 2015 and 2020 for VHI**

VHI	2000		2005		2010		2015		2020	
	Area in Sq.km	Area(%)	Area in Sq.km	Area(%)	Area in Sq.km	Area(%)	Area in Sq.km	Area(%)	Area in Sq.km	Area(%)
Extreme drought	587.41	20	90.32	3	752.70	25	843.03	28	30.11	1
Severe drought	270.97	9	632.27	21	1023.68	34	602.16	20	873.13	29
Moderate drought	358.59	12	812.92	27	632.27	21	963.46	32	752.70	25
Mild drought	503.41	17	993.57	33	270.97	9	331.19	11	632.27	21
No drought	1289.23	43	541.95	18	331.19	11	270.97	9	722.59	24
<b>Total</b>	<b>3010.81</b>	<b>100</b>	<b>3010.81</b>	<b>100</b>	<b>3010.81</b>	<b>100</b>	<b>3010.81</b>	<b>100</b>	<b>3010.81</b>	<b>100</b>



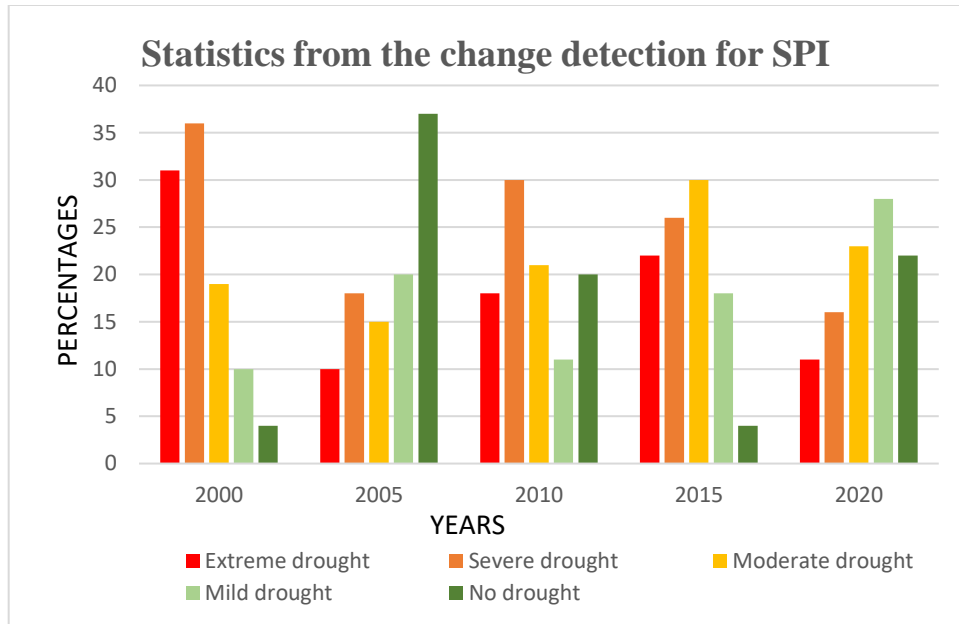


**Figure 11: Statistics from change detection for SPI**

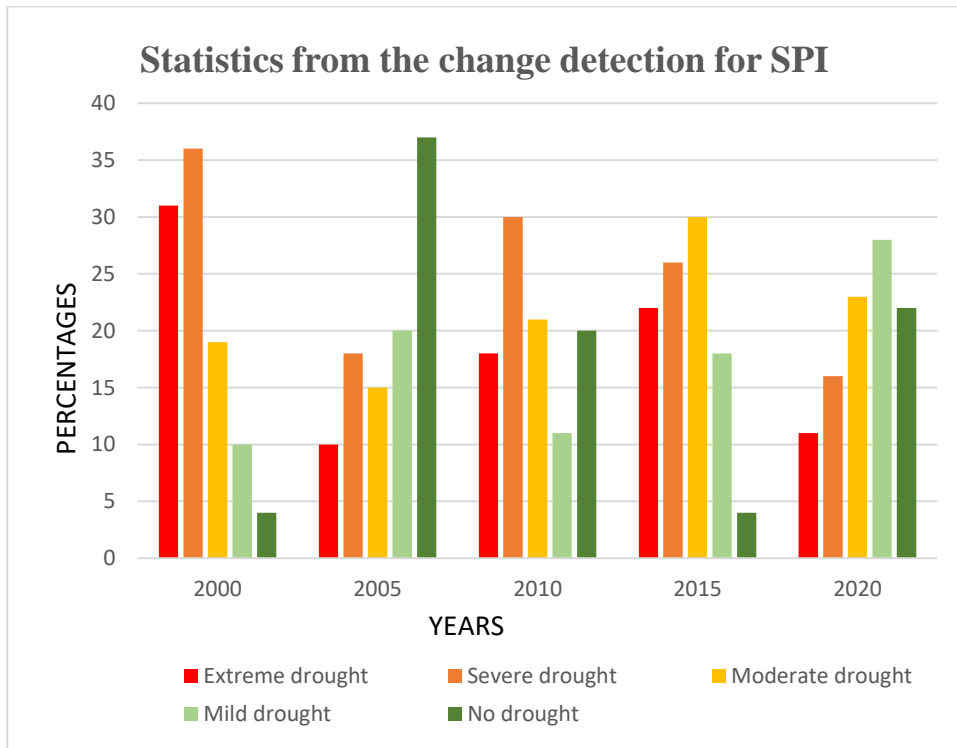


**Figure 12: Statistics from change detection for VHI**

The graphs above show by what percentage drought was changing in Isingiro district from 2000 to 2020 at a five-year interval according to the different classes of drought created. From the graphs 2000 and 2015 were the driest years and for 2005 and 2020 the drought was mild.

#### 4.2.4 Analysis of the relationship between SPI and VHI

SPI-3 and VHI-2010 have the lowest correlation of 0.105 at the 3-month time scale and the highest correlation is in 2000(0.541) and 2015(0.659). VHI shows more areas affected by drought compared to SPI. The comparative analysis of the two indices indicated that VHI and SPI are highly correlated in the years 2000 and 2015. Drought analysis based on these indices showed that for drought assessment VHI can be used to depict drought condition of the study area more realistically. The results of this comparison show that 12-month scale of SPI and VHI have a higher correlation. Overall SPI-12 had the highest correlations with VHI data. VHI-2015 and SPI-12 had the highest correlation coefficient of 0.659. Hence, the 6-month timescale is better when using SPI to monitor drought.

*Table 5: Correlation coefficients between VHI and SPI*

<b>INDICES</b>	<b>SPI-3</b>	<b>SPI-6</b>	<b>SPI-12</b>
<b>VHI-2000</b>	0.386	0.457	0.551
<b>VHI-2005</b>	0.443	0.397	0.473
<b>VHI-2010</b>	0.105	0.313	0.255
<b>VHI-2015</b>	0.393	0.403	0.659
<b>VHI-2020</b>	0.337	0.319	0.478

## **CHAPER FIVE: CONCLUSION AND RECOMMENDATION**

### **5.1 Introduction**

This chapter presents the conclusion and recommendations, which are based on the findings of the study.

### **5.2 Conclusion**

The VHI and SPI indices were used to identify the temporal and spatial drought patterns as derived from the study of a 20-year time period. The analysis revealed that 2000 and 2015 were the driest years. Using SPI, the southeastern and northwestern parts of the Isingiro district are the areas that are susceptible to drought and while using VHI, it was the northwestern, southwestern and southwestern parts of Isingiro are the areas that are susceptible to drought. SPI works well when there is an even distribution of weather stations in the area.

SPI-3 and VHI-2010 had the lowest correlation of 0.105 at the 3-month time scale and the highest correlation was in 2000(0.541) and 2015(0.659). VHI showed more areas affected by drought compared to SPI. The comparative analysis of the two indices indicated that VHI and SPI are highly correlated in the years 2000 and 2015. Drought analysis based on these indices showed that for drought assessment VHI can be used to depict drought condition of the study area more realistically. The results of this comparison show that 12-month scale of SPI and VHI have a higher correlation.

### **5.3 Recommendations**

Based on the findings of this research, it's recommended that Standardized Precipitation Index should only be used where sufficient data collected on precipitation is available and has enough instrumentation and where you don't have sufficient precipitation data and enough instrumentation it's better to use Vegetation Health Index.

## REFERENCES

- Abood, R. H. and Mahmoud, R. R. (2018) 'Drought assessment using GIS and meteorological data in Maysan province /Iraq', *International Journal of Civil Engineering and Technology*, 9(6), pp. 516–524.
- Abuzar, M. K. *et al.* (2017) 'Drought risk assessment using GIS and remote sensing: A case study of District Khushab, Pakistan', ... *and Technology* ..., (September). Available at: [https://cest.gnest.org/sites/default/files/presentation\\_file\\_list/cest2017\\_00658\\_oral\\_paper.pdf](https://cest.gnest.org/sites/default/files/presentation_file_list/cest2017_00658_oral_paper.pdf).
- Abuzar, M. K. *et al.* (2019) 'Drought Risk Assessment in the Khushab Region of Pakistan Using Satellite Remote Sensing and Geospatial Methods', *International Journal of Economic and Environmental Geology*, 10(1), pp. 48–56. doi: 10.46660/ojs.v10i1.217.
- Achite, M. *et al.* (2022) 'Forecasting of SPI and SRI Using Multiplicative ARIMA under Climate Variability in a Mediterranean Region: Wadi Ouahrane Basin, Algeria', *Climate*, 10(3). doi: 10.3390/cli10030036.
- Agwata (2014) 'A Review of Some Indices used for Drought Studies', *Civil and Environmental Research*, 6(2), pp. 14–21. Available at: <http://www.iiste.org/Journals/index.php/CER/article/view/10842%0Ahttps://www.uonbi.ac.ke/agwatas/files/10842-13144-1-pb.pdf%5Cnhttp://www.iiste.org/Journals/index.php/CER/article/view/10842/11145>.
- Asokan, A. *et al.* (2020) 'applied sciences Image Processing Techniques for Analysis of Satellite Images for Historical Maps Classification — An Overview'.
- Aswathi, P. V. *et al.* (2018) 'Assessment and monitoring of agricultural droughts in Maharashtra using meteorological and remote sensing based indices', *ISPRS Annals of the Photogrammetry, Remote Sensing and Spatial Information Sciences*, 4(5), pp. 253–264. doi: 10.5194/isprs-annals-IV-5-253-2018.
- Bayissa, Y. A. *et al.* (2019) 'Developing a satellite-based combined drought indicator to monitor agricultural drought: a case study for Ethiopia', *GIScience and Remote Sensing*, 56(5), pp. 718–748. doi: 10.1080/15481603.2018.1552508.

- Belal, A. A. *et al.* (2014) 'Drought risk assessment using remote sensing and GIS techniques', *Arabian Journal of Geosciences*, 7(1), pp. 35–53. doi: 10.1007/s12517-012-0707-2.
- Bera, S. *et al.* (2018) 'Using Remote Sensing and GIS Techniques for Drought Monitoring of Purulia District , West Bengal-', 6(1), pp. 707–717.
- Chopra, P. (2006) 'Drought risk assessment using remote sensing and GIS: a case study of Gujarat', *International Journal of Disaster Risk Science*, 4(3), pp. 1–38. Available at: [http://www.itc.nl/library/papers\\_2006/msc/iirs/chopra.pdf%0Apapers2://publication/uuid/A67C6FF4-8625-493A-9266-2BC7F3F2CF0A%0Ahttp://www.mdpi.com/2227-7099/4/3/19](http://www.itc.nl/library/papers_2006/msc/iirs/chopra.pdf%0Apapers2://publication/uuid/A67C6FF4-8625-493A-9266-2BC7F3F2CF0A%0Ahttp://www.mdpi.com/2227-7099/4/3/19).
- Cristóbal, J. *et al.* (2009) 'Improvements in land surface temperature retrieval from the Landsat series thermal band using water vapor and air temperature', *Journal of Geophysical Research Atmospheres*, 114(8), pp. 1–16. doi: 10.1029/2008JD010616.
- Dutta, D. *et al.* (2015) 'Assessment of agricultural drought in Rajasthan (India) using remote sensing derived Vegetation Condition Index (VCI) and Standardized Precipitation Index (SPI)', *Egyptian Journal of Remote Sensing and Space Science*, 18(1), pp. 53–63. doi: 10.1016/j.ejrs.2015.03.006.
- Foody, G. M. (2002) 'Status of land cover classification accuracy assessment', 80, pp. 185–201.
- Ghobadi, Y. *et al.* (2015) 'Assessment of spatial relationship between land surface temperature and landuse/cover retrieval from multi-temporal remote sensing data in South Karkheh Sub-basin, Iran', *Arabian Journal of Geosciences*, 8(1), pp. 525–537. doi: 10.1007/s12517-013-1244-3.
- Goetz, S. J. (1997) 'Multi-sensor analysis of NDVI, surface temperature and biophysical variables at a mixed grassland site', *International Journal of Remote Sensing*, 18(1), pp. 71–94. doi: 10.1080/014311697219286.
- Hammouri, N. and El-Naqa, A. (2007) 'Drought assessment using GIS and remote sensing in Amman-Zarqa Basin, Jordan', *Jordan Journal of Civil Engineering*, 1(2), pp. 142–152.
- Hänsel, S., Schucknecht, A. and Matschullat, J. (2016) 'The Modified Rainfall Anomaly Index (mRAI)—is this an alternative to the Standardised Precipitation Index (SPI) in evaluating future extreme precipitation characteristics?', *Theoretical and Applied Climatology*, 123(3–4), pp. 827–844. doi: 10.1007/s00704-015-1389-y.

Hao, Z. *et al.* (2018) 'Changes in the severity of compound drought and hot extremes over global land areas', *Environmental Research Letters*, 13(12). doi: 10.1088/1748-9326/aace96.

Himanshu, S. K., Singh, G. and Kharola, N. (2015) 'Monitoring of drought using satellite data', *International Research Journal of Earth Sciences*, 3(1), pp. 66–72.

Jeyaseelan, A. T. (no date) 'DROUGHTS & FLOODS ASSESSMENT AND MONITORING USING REMOTE SENSING AND GIS', pp. 291–313.

Jimenez-Munoz, J. C. *et al.* (2009) 'Revision of the single-channel algorithm for land surface temperature retrieval from landsat thermal-infrared data', *IEEE Transactions on Geoscience and Remote Sensing*, 47(1), pp. 339–349. doi: 10.1109/TGRS.2008.2007125.

Karnieli, A. *et al.* (2010) 'Use of NDVI and land surface temperature for drought assessment: Merits and limitations', *Journal of Climate*, 23(3), pp. 618–633. doi: 10.1175/2009JCLI2900.1.

Lazaridou.M. A. & Karagianni A. Ch. (2016) 'LANDSAT 8 MULTISPECTRAL AND PANSHARPENED IMAGERY PROCESSING ON THE STUDY OF CIVIL ENGINEERING ISSUES', XLI(July), pp. 941–945. doi: 10.5194/isprsarchives-XLI-B8-941-2016.

Lineament, S. *et al.* (2012) 'Landsat ETM + 7 Digital Image Processing Techniques for Lithological and Landsat ETM + 7 Digital Image Processing Techniques for Lithological and Structural Lineament Enhancement: Case Study Around Abidiya Area ', (May 2014). doi: 10.2174/1875413901205010083.

Mekonen, A. A., Berlie, A. B. and Ferede, M. B. (2020) 'Spatial and temporal drought incidence analysis in the northeastern highlands of Ethiopia', *Geoenvironmental Disasters*, 7(1). doi: 10.1186/s40677-020-0146-4.

Meteorological, W. *et al.* (1906) *West Australia, British Medical Journal*. doi: 10.1136/bmj.1.2366.1068-b.

Mlenga, D. H., Jordaan, A. J. and Mandebvu, B. (2019) 'Monitoring droughts in Eswatini: A spatiotemporal variability analysis using the Standard Precipitation Index', *Jamba: Journal of Disaster Risk Studies*, 11(1), pp. 1–11. doi: 10.4102/JAMBA.V11I1.725.

Morid, S., Smakhtin, V. and Moghaddasi, M. (2006) 'Comparison of seven meteorological indices

for drought monitoring in Iran’, *International Journal of Climatology*, 26(7), pp. 971–985. doi: 10.1002/joc.1264.

Ntale, H. K., Gan, T. Y. and Mwale, D. (2003) ‘Prediction of East African seasonal rainfall using simplex canonical correlation analysis’, *Journal of Climate*, 16(12), pp. 2105–2112. doi: 10.1175/1520-0442(2003)016<2105:POEASR>2.0.CO;2.

Patil, M. B., Desai, C. G. and Umrikar, and \*Bhavana N. (2012) ‘IMAGE CLASSIFICATION TOOL FOR LAND USE / LAND COVER ANALYSIS : A COMPARATIVE STUDY OF MAXIMUM LIKELIHOOD’, 2(3), pp. 189–196.

Qin, Z., Karnieli, A. and Berliner, P. (2001) ‘A mono-window algorithm for retrieving land surface temperature from Landsat TM data and its application to the Israel-Egypt border region’, *International Journal of Remote Sensing*, 22(18), pp. 3719–3746. doi: 10.1080/01431160010006971.

Quiring, S. M. (2009) ‘Developing objective operational definitions for monitoring drought’, *Journal of Applied Meteorology and Climatology*, 48(6), pp. 1217–1229. doi: 10.1175/2009JAMC2088.1.

Rimkus, E. *et al.* (2017) ‘Drought identification in the eastern Baltic region using NDVI’, *Earth System Dynamics*, 8(3), pp. 627–637. doi: 10.5194/esd-8-627-2017.

Senay, G. B. *et al.* (2014) *Drought Monitoring and Assessment: Remote Sensing and Modeling Approaches for the Famine Early Warning Systems Network. Remote Sensing and Modeling Approaches for the Famine Early Warning Systems Network., Hydro-Meteorological Hazards, Risks, and Disasters.* doi: 10.1016/B978-0-12-394846-5.00009-6.

Shah, R., Bharadiya, N. and Manekar, V. (2015) ‘Drought Index Computation Using Standardized Precipitation Index (SPI) Method For Surat District, Gujarat’, *Aquatic Procedia*, 4(Icwrcoe), pp. 1243–1249. doi: 10.1016/j.aqpro.2015.02.162.

Sholihah, R. I. *et al.* (2016) ‘Identification of Agricultural Drought Extent Based on Vegetation Health Indices of Landsat Data: Case of Subang and Karawang, Indonesia’, *Procedia Environmental Sciences*, 33, pp. 14–20. doi: 10.1016/j.proenv.2016.03.051.

Singh, R. P., Roy, S. and Kogan, F. (2003) ‘Vegetation and temperature condition indices from

NOAA AVHRR data for drought monitoring over India’, *International Journal of Remote Sensing*, 24(22), pp. 4393–4402. doi: 10.1080/0143116031000084323.

Sowmya, D. R. (2020) ‘Remote Sensing Satellite Image Processing Techniques for Image Remote Sensing Satellite Image Processing Techniques for Image Classification : A Comprehensive Survey’, (August). doi: 10.5120/ijca2017913306.

Sruthi, S. and Aslam, M. A. M. (2015) ‘Agricultural Drought Analysis Using the NDVI and Land Surface Temperature Data; a Case Study of Raichur District’, *Aquatic Procedia*, 4(Icwrcoe), pp. 1258–1264. doi: 10.1016/j.aqpro.2015.02.164.

Sun, D. and Kafatos, M. (2007) ‘Note on the NDVI-LST relationship and the use of temperature-related drought indices over North America’, *Geophysical Research Letters*, 34(24). doi: 10.1029/2007GL031485.

Svoboda, M. and Fuchs, B. (2017) *Handbook of Drought Indicators and Indices\**. doi: 10.1201/9781315265551-12.

Thenkabail, P. S., Gamage, M. S. D. N. and Smakhtin, V. U. (2004) *The use of remote sensing data for drought assessment and monitoring in southwest Asia, IWMI Research Report 085*.

Thomas B. McKee, N. J. D. and J. K. (1993) ‘THE RELATIONSHIP OF DROUGHT FREQUENCY AND DURATION TO TIME SCALES’, *Journal of Surgical Oncology*, 105(8), pp. 818–824. doi: 10.1002/jso.23002.

‘TITLE PAGE Running Head’: (2017). doi: 10.1111/ijlh.12426.

Tsakiris, G. and Vangelis, H. (2005) ‘Establishing a drought index incorporating evapotranspiration’, *European Water*, 9(10), pp. 3–11.

Vikram Agone, S. M. B. (2008) ‘Change Detection of Vegetation Cover, using Multi-Temporal Remote Sensing Data and GIS Techniques.’, *37th COSPAR Scientific Assembly*, (1978), pp. 1–5. Available at: <http://adsabs.harvard.edu/abs/2008cosp...37...26A>.

Vogt, J. V. *et al.* (2018) *Drought Risk Assessment and Management. A conceptual framework, EUR 29464 EN, Publications Office of the European Union*. doi: 10.2760/057223.

Wilhite, D. A. (2021) ‘Drought As a Natural Hazard’, *Droughts*, pp. 33–33. doi:



10.4324/9781315830896-24.

Wilhite et al (1987) 'The Role of Definitions Understanding : the Drought Phenomenon : The Role of Definitions \*', *Westview Press*, (August 2013), pp. 11–27.

宗成庆 (no date) 'No Title统计自然语言处理 ( 第二版 ) '.

Wilhite , D. & Glantz , H. M., 1985. Understanding the Drought phenomenon. The role of definitions, Volume 10, pp. 111-120.

Young, N. E., Anderson, R., Chignell, S., & Vorster, A. (2017). CONCEPTS & SYNTHESIS.